

## Research Article

# Groundwater quality evaluation for irrigation using irrigation water quality indexes under GIS framework in Aksum Area, Northern Ethiopia

Haile Tadelle Abadi<sup>1\*</sup>, Weldegebriel Haile<sup>1</sup>, Negasi Gebremedhin<sup>2</sup>

<sup>1</sup> Department of Geology, Faculty of Mines, Aksum University, Shire, Ethiopia.

<sup>2</sup> School of Earth Sciences, College of Natural and Computational Sciences, Mekelle University, Mekelle, Tigray, Ethiopia.

**Abstract:** This study evaluates the suitability of irrigation water in the semi-arid region of Aksum, northern Ethiopia. An integrated approach combining the Irrigation Water Quality Index (IWQI) and ArcGIS-based spatial analysis was applied to assess the spatial variability of irrigation water quality. Twenty-five groundwater samples were collected and analyzed for key physicochemical parameters and heavy metals using standard laboratory techniques. Exceedances of recommended irrigation water limits were recorded for magnesium (16%), nitrate (32%), salinity hazard (12%), total dissolved solids (20%), total hardness (60%), residual sodium carbonate (16%), kelly index (4%), and magnesium ratio (32%). Based on the Irrigation Water Quality Index (IWQI), 36% of the samples fell under high restriction, 32% under moderate restriction, 24% under severe restriction, and 8% under low restriction for irrigation use. Although most of groundwater sources are suitable based on individual water quality parameters, the IWQI indicates that a significant portion of samples requires restricted use for irrigation. This highlights the need for targeted groundwater management strategies to mitigate localized risks associated with salinity and sodicity. The integrated IWQI-GIS approach demonstrated in this study is readily transferable to other arid and semi-arid regions, providing a robust tool for sustainable irrigation management and climate-resilient agricultural planning.

**Keywords:** Hydrogeochemistry; Spatial analysis; Irrigation water suitability; Agricultural water management; Semi-arid climate; IWQI

Received: 25 Jan 2025/ Accepted: 17 Dec 2025/ Published: 30 Apr 2026

## Introduction

Water is one of the planet's most vital natural resources, essential for life and human activity. In areas with limited rainfall, such as arid and semi-arid regions, water scarcity and contamination have a significant impact on agricultural productivity (Tian et al. 2025; Djafer et al. 2024; Aida et al. 2024). Salinity and contamination, whether from

natural or anthropogenic sources, exacerbate soil salinization (He et al. 2025), particularly in regions with high temperatures and inadequate water supply (Palmate et al. 2022; Tomaz et al. 2020; Eswar et al. 2021). Poor-quality irrigation water can lead to reduced crop yields, soil degradation, and damage to irrigation infrastructure due to salinity and toxicity, even though minerals in water are crucial for plant growth (Tarolli et al. 2024). Therefore, evaluating the chemical and physical characteristics of irrigation water is critical for maintaining sustainable agricultural practices (Gurmesa et al. 2022).

In developing nations, especially in Africa, where agriculture is a cornerstone of livelihoods, assessing irrigation water quality is essential. Countries such as Egypt, Kenya, and South Africa have adopted the Irrigation Water Quality Index (IWQI) to evaluate the suitability of water for agri-

\*Corresponding author: Haile Tadelle Abadi, *E-mail address:* [hailetadele2009@gmail.com](mailto:hailetadele2009@gmail.com)

DOI: 10.26599/JGSE.2026.9280075

Abadi HT, Haile W, Gebremedhin N. 2026. Groundwater quality evaluation for irrigation using irrigation water quality indexes under GIS framework in Aksum Area, Northern Ethiopia. *Journal of Groundwater Science and Engineering*, 14(2): 123-147.

2305-7068/© 2026 Journal of Groundwater Science and Engineering Editorial Office. This is an open access article under the CC BY-NC-ND license (<http://creativecommons.org/licenses/by-nc-nd/4.0>)

cultural purposes (El-Rawy et al. 2023). For instance, IWQI applications in Kenya have revealed groundwater challenges, including contamination and over-extraction caused by agricultural runoff (Mutemi et al. 2017). Salinity remains a significant issue in Africa, affecting approximately 80 million hectares, with around 69 million hectares located in sub-Saharan regions. Globally, salinity is projected to impact over half of the world's agricultural land by 2050, resulting in annual economic losses of US Dollar 12 billion (Kebede et al. 2023). In Ethiopia, salinity and alkalinity threaten approximately 75 million hectares of arid to semi-arid land (Debela, 2017).

Due to the importance of irrigation in Ethiopia's agricultural sector, particularly in arid and semi-arid regions, water quality assessments are crucial. Previous studies in Ethiopia, including in the Tigray region, have focused on water exploration and evaluating physicochemical characteristics. For example, Berhe and Letab (2015), Tadesse et al. (2011), Nedaw (2010), Mehari and Hailu (2019), and Tadesse et al. (2009) examined irrigation water quality in the Tigray region. Such studies often lack a comprehensive approach that integrates multiple parameters into a single, easily interpretable value for informed decision-making.

Globally, individual irrigation water quality parameters such as Sodium Adsorption Ratio (SAR), Electrical Conductivity (EC), and Residual Sodium Carbonate (RSC) have traditionally been used to assess irrigation water quality. While these parameters provide useful insights, they represent a conventional approach. Recently, tools such as the Irrigation Water Quality Index (IWQI) have gained prominence, as they integrate multiple parameters into a single value, thereby simplifying complex data and supporting more effective decision-making (Masoud et al. 2022). IWQI has been successfully applied in countries such as China, India, and the United States, demonstrating its utility for water management in arid and semi-arid regions (Wahyuningsih et al. 2023; Saad et al. 2023; Abadi et al. 2024).

In northern Ethiopia, particularly the Aksum area, rain-fed agriculture is the dominant farming system but remains highly vulnerable due to erratic and insufficient rainfall. Consequently, farmers increasingly depend on groundwater-based supplemental irrigation to maintain crop yields and enhance productivity. However, in the Aksum area, research related to water quality for irrigation is scant. Therefore, inadequate irrigation management and the use of water with unsuitable chemical characteristics can lead to soil saliniza-

tion, fertility loss, and land degradation (Berhe et al. 2022; Abadi et al. 2024). Many studies worldwide, and most of the studies carried out in Ethiopia, have focused on standard irrigation water quality assessments, which often examine individual parameters in isolation and are inadequate for sustainable management.

To address this, the present study integrates the Irrigation Water Quality Index (IWQI) with multiple specific hazard indices, such as sodium adsorption ratio, residual sodium carbonate, magnesium ratio, sodium percentage, permeability index, potential salinity, and Kelly index, within a GIS-based spatial analysis framework. Groundwater samples were collected and analyzed for key physicochemical parameters and heavy metals, with quality control ensured through ionic balance checks, standard solutions, and blanks (Gad et al. 2021; Batarseh et al. 2021). This combined approach not only provides a comprehensive and spatially explicit evaluation of irrigation water suitability but also supports evidence-based decision-making for farmers and water managers (Ayers and Westcot, 1985; Meireles et al. 2010). The methodology offers a replicable model for arid and semi-arid regions worldwide, delivering both environmental protection and agricultural productivity gains while addressing the unique challenges faced in the Aksum area.

## 1 Study area

The study was conducted in the historic city of Aksum, located in the Central Zone of Tigray regional state, northern Ethiopia (Figs. 1a, 1b). Aksum is located about 245 km northwest of Mekelle, the region's capital (Fig. 1b). Geographically, the area lies between 456,000–476,000 m E and 1,548,000–1,564,000 m N (Fig. 1c) and is situated on a mountain ridge. The study area encompasses many perennial and seasonal rivers such as Mysiye, Dura, Arekeyti, Kowoh and Debrebrhan Rivers (Fig. 1c).

Aksum is characterized by a varied topography, including hilly landscapes and flat plateaus, with the town surrounded by mountain hills on its north, east, and west sides. The altitudes of the area range from 1,832 m to 2,475 m above sea level (Fig. 1d). To examine the spatial variation of groundwater quality with respect to elevation, the study area was classified into five elevation zones using a Digital Elevation Model (DEM) processed in ArcGIS. The classification was done purposively rather than using fixed statistical or natural break

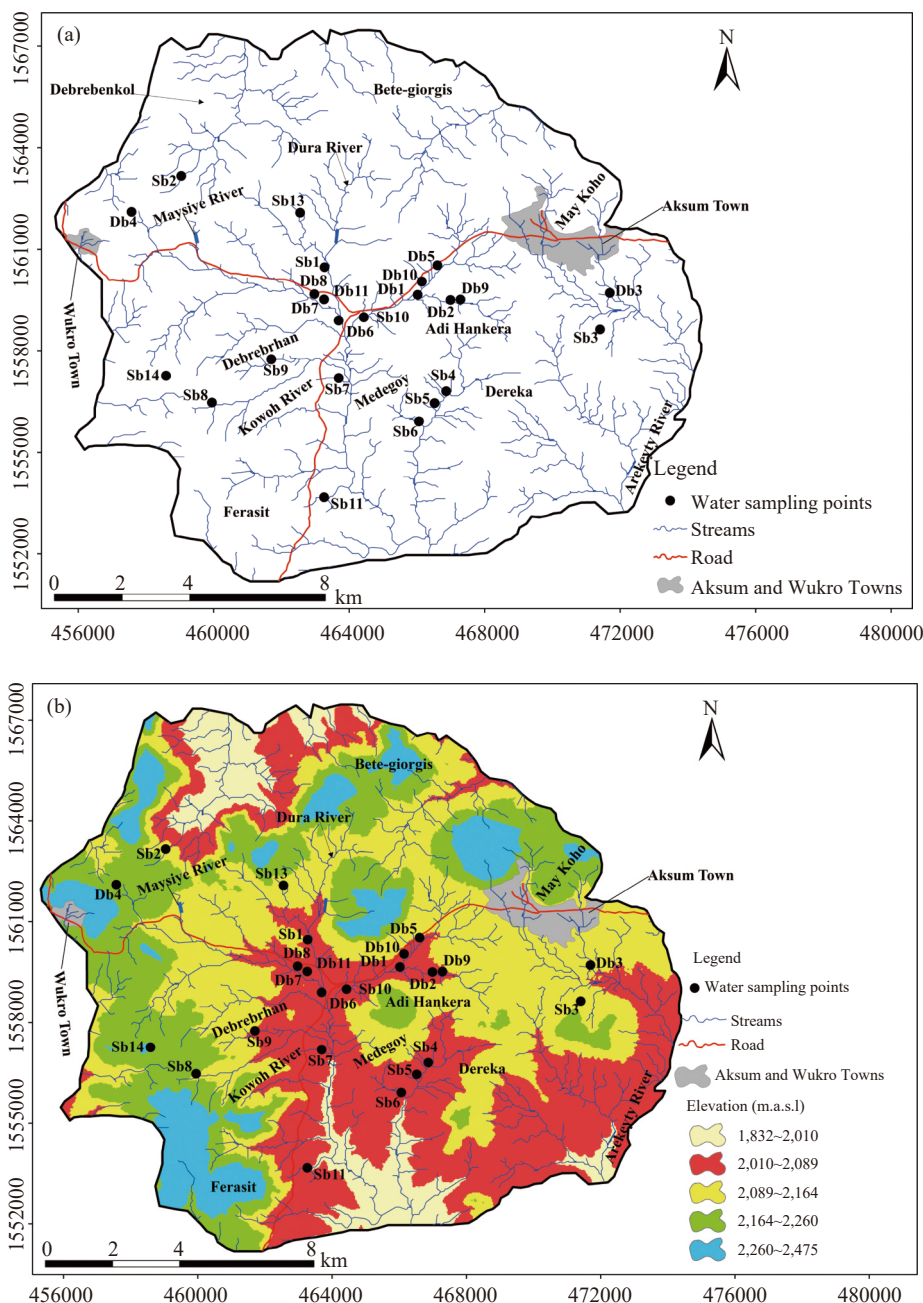


**Fig. 1** Location and physiographic map of the study area

(a) Study area showing groundwater sampling points, streams and other water bodies; (b) Physiographic map of the study area.

methods. This approach was adopted to capture meaningful topographic differences relevant to hydrogeochemical processes, such as recharge potential, flow direction, and water-rock interactions. The zonation facilitates a clearer interpretation of hydrogeochemical variations along elevation gradients within the volcanic terrain.

The geomorphology of the area reflects influences from Quaternary sedimentary deposits and volcanic activity. Its drainage pattern is dendritic, with streams generally flowing from north to south. The area has a semi-arid climatic condition with an average annual temperature of 19.8°C and

an average annual rainfall of 670 mm. Over 80% of rainfall occurs between June and September, with a peak in August.

### 1.1 Land Use Land Cover (LULC)

The LULC analysis of the study area identified five distinct land cover classes: Agricultural land, vegetation, bare land, settlements, and water bodies. Among these, agricultural land accounts for the largest portion, covering approximately 41% of the total area (Fig. 2). This dominant coverage reflects that the region's crop cultivation

and land-based livelihoods are the primary economic activities. The significant extent of agricultural land suggests intensive land use and pressure on natural ecosystems, particularly in the absence of sustainable land management practices. Vegetation-covered areas make up 31.9% of the land, representing natural vegetation such as eucalyptus, shrubs, and bushes. This class plays an essential role in maintaining ecological balance, providing habitats, and contributing to soil and water conservation. However, the presence of 19% bare land areas with minimal or no vegetation indicates environmental degradation, likely driven by deforestation, overgrazing, or soil erosion, which are common in semi-arid highland regions of northern Ethiopia. Settlement areas occupy 8% of the total land area, reflecting the growing expansion of rural towns and villages. The increasing built-up area may be associated with population growth and infrastructure development, which could further exert pressure on nearby agricultural and vegetated lands if not properly planned. Water bodies constitute only 0.1% of the study area, indicating limited surface water availability. This minimal coverage of water resources may pose challenges for irrigation, livestock watering, and domestic water supply, particularly during dry seasons. It highlights the need for sustainable water resource management.

Overall, the LULC composition highlights a landscape predominantly shaped by agricultural activities and natural vegetation, human settlement, and environmentally vulnerable bare lands. These findings can inform land use planning, environmental management, and policy decisions aimed at balancing development with resource conservation. Because land use and land cover changes directly affect soil erosion, infiltration, and contaminant loading, it is also important to consider the spatial distribution of soil types in the catchment. In what follows, the soil characteristics of the study area and their implications for groundwater recharge and quality are described.

### 1.2 Soil characteristics

The soils of the study area exhibit considerable spatial variability (Fig. 3). The northern and south-eastern parts are dominated by clay and sandy clay loam. In contrast, the central part is covered by silt clay. Clay and silt clay loam are the most extensive soil types, covering 27.02% and 26.79% of the total area, respectively. Other soil types include sandy clay loam (22.93%), silt clay (17.19%), and areas with thin or absent soil (6.07%) (Fig. 3). Soil texture and permeability strongly influence recharge, infiltration, and contaminant attenuation:

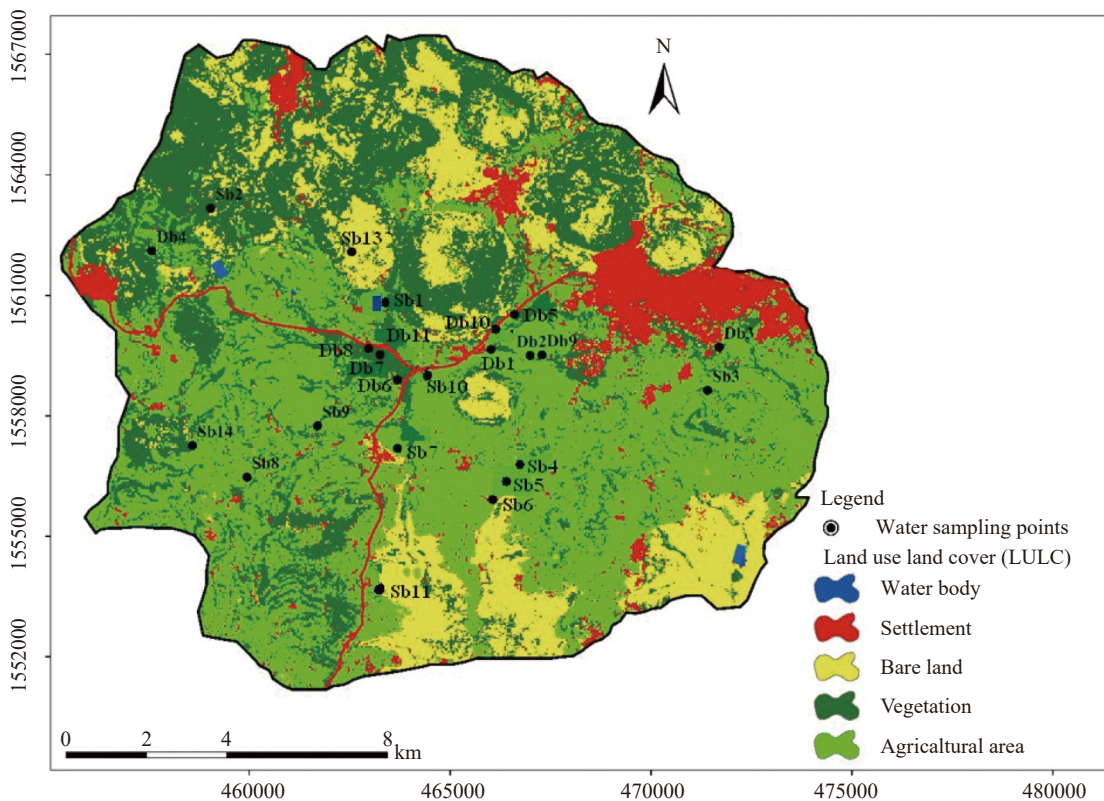
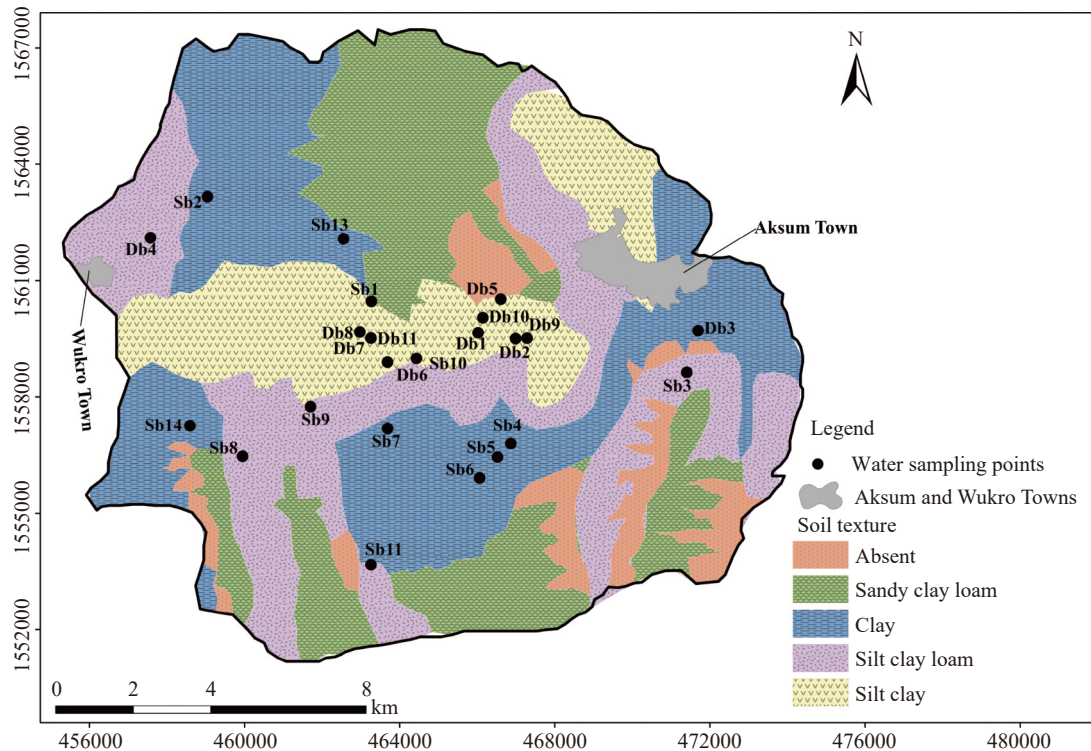


Fig. 2 Land use and land cover (LULC) map of the study area



**Fig. 3** Soil characteristics (texture) of the study area

Coarse-textured soils enhance infiltration, whereas fine-textured soils restrict it (Mkumbo et al. 2022). Therefore, these spatial variations in soil texture and permeability are expected to influence groundwater recharge, flow, and contaminant transport in the catchment. To place these soil controls within a broader subsurface framework, the geological and hydrogeological conditions that determine aquifer properties and groundwater occurrence in the study area are examined next.

### 1.3 Geology and hydrogeological conditions

The geology of the Aksum area is characterized by rocks ranging in age from Precambrian bedrock to Quaternary deposits. The area is predominantly covered by Tertiary flood basalts, with minor occurrences of phonolite plugs, trachyte, sandstone, and Quaternary sediments (Hagos et al. 2020) (Fig. 4). Paleosol, mudstone, gravel, and alluvial deposits cover the agricultural areas, while reddish sandstone overlies the Precambrian bedrock unconformably. Weathering of the upper basalt layers has created extensive clay blankets, while phonolite and trachyte form steep, circular hills due to their resistance to erosion.

The hydrogeological system of the Aksum area is shaped by the interaction of lithology, structure, and geomorphology, which control aquifer occur-

rence, productivity, and groundwater flow. Based on transmissivity values and well productivity data, the aquifers of Aksum are classified into three generalized categories (Fig. 5):

Moderately permeable aquifers include highly fractured and weathered basalts, weathered phonolite, and localized alluvial deposits. These aquifers, though variable in yield, can supply small communities. The average transmissivity value is approximately  $37 \text{ m}^2/\text{d}$ .

Low-permeability aquifers comprise slightly weathered basalts, sandstone intercalated with siltstone, and basalts clogged with clay or secondary precipitates. These are mainly found in plain topography and are only suitable for small-scale or private water supply. Average transmissivity is approximately  $8.8 \text{ m}^2/\text{d}$ .

Very low permeable aquifers include massive basalt, compact trachyte, poorly fractured sandstone, and mudstone. These units are characterized by low groundwater potential, acting more as runoff or confining zones, and transmissivity is typically  $< 1 \text{ m}^2/\text{d}$ .

Well yields of the area also reflect this heterogeneity. Fractured basalt and alluvial aquifers provide 5–15 L/s, while sandstone and basalt intercalations yield  $< 2.5 \text{ L/s}$  and are susceptible to drying. According to Devecon Engineers and Architects (1995), groundwater recharge in the basin, estimated by the Darcian method, is about  $4,600 \text{ m}^3/\text{d}$ . Literature suggests that only approxi-

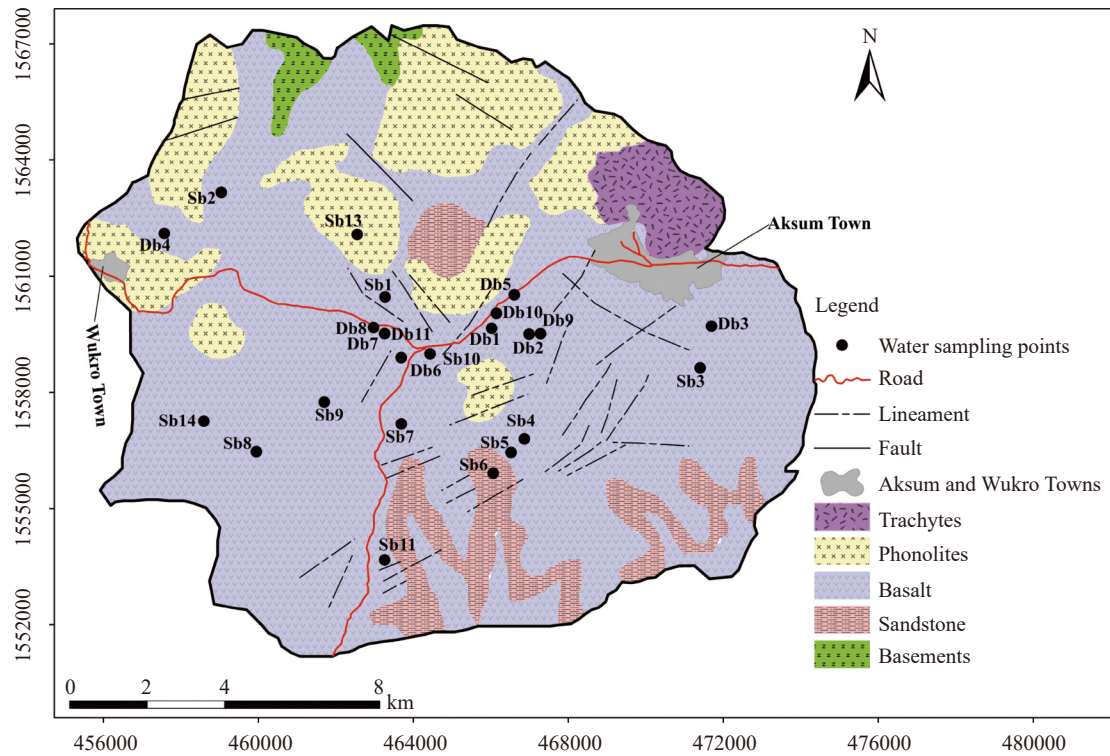


**Fig. 4** Geological map of the study area with sampling points and major geological structure

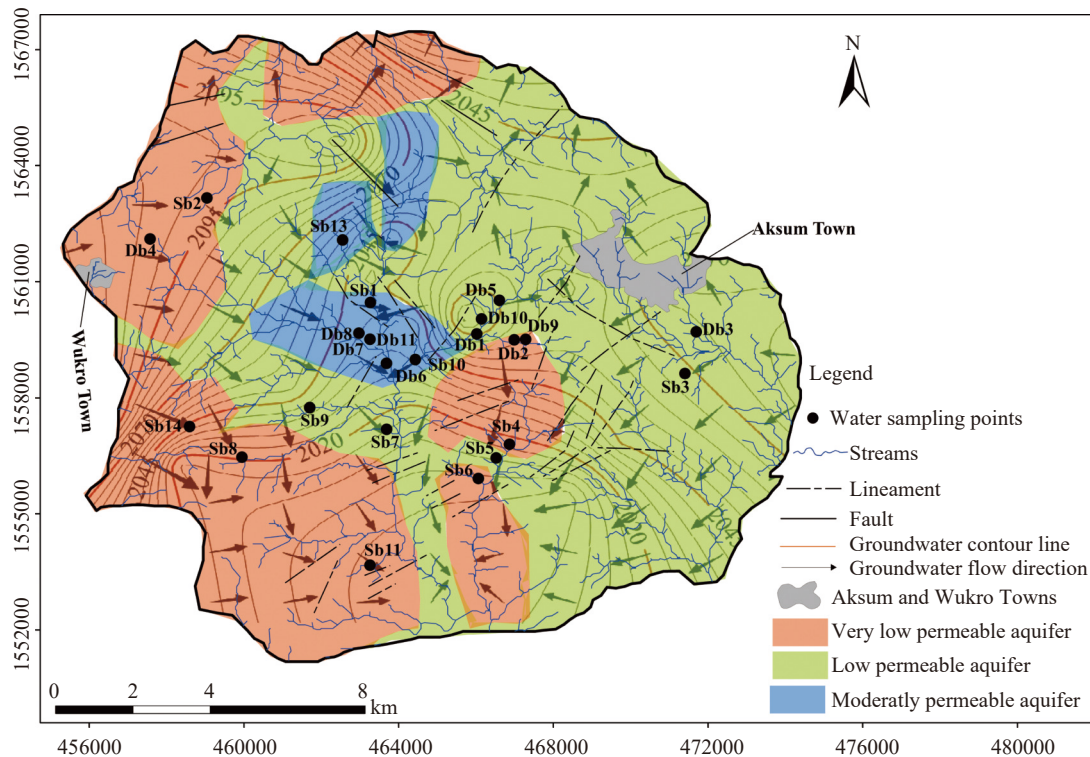


**Fig. 5** Hydrogeological map of the study area

mately 20% of the total recharge is economically exploitable, which equates to approximately 920 m<sup>3</sup>/d. However, current abstraction is around 1,320 m<sup>3</sup>/d, exceeding sustainable limits. This overex-

ploitation has resulted in declining water tables and the drying of wells.

Groundwater flow in the Aksum area broadly follows the topographic gradient, moving from the

northern escarpments toward the southern plains. Structural discontinuities such as faults, fractures, and lineaments strongly influence groundwater occurrence and flow. These features act as preferential pathways that enhance infiltration and groundwater circulation in weathered and fractured zones, especially within basalts and phonolites. In some cases, however, dykes and fault zones act as barriers to groundwater flow, producing perched systems or localized variations in yield and water quality. This explains why neighboring wells, such as Sb9 and Sb3, exhibit significant differences in productivity and water chemistry despite being drilled into similar formations.

The alignment of productive wells along major lineaments demonstrates the importance of structural control, while wells located away from these features often show poor yields. The generalized subsurface aquifer characterization was carried out

by using outcrop geological observation data and borehole logs. The borehole log data reveal heterogeneity in aquifer type, vertical thickness variation, and extent (Fig. 6). These geological and hydrogeological characteristics exert primary control on groundwater occurrence, flow paths, and water-rock interactions, and therefore strongly influence groundwater quality and its suitability for irrigation. On this basis, the groundwater sampling strategy and analytical methods used to evaluate groundwater suitability in the study area are presented.

## 2 Materials and methods

### 2.1 Water sampling

Groundwater sampling points were strategically selected based on detailed GIS analysis and field

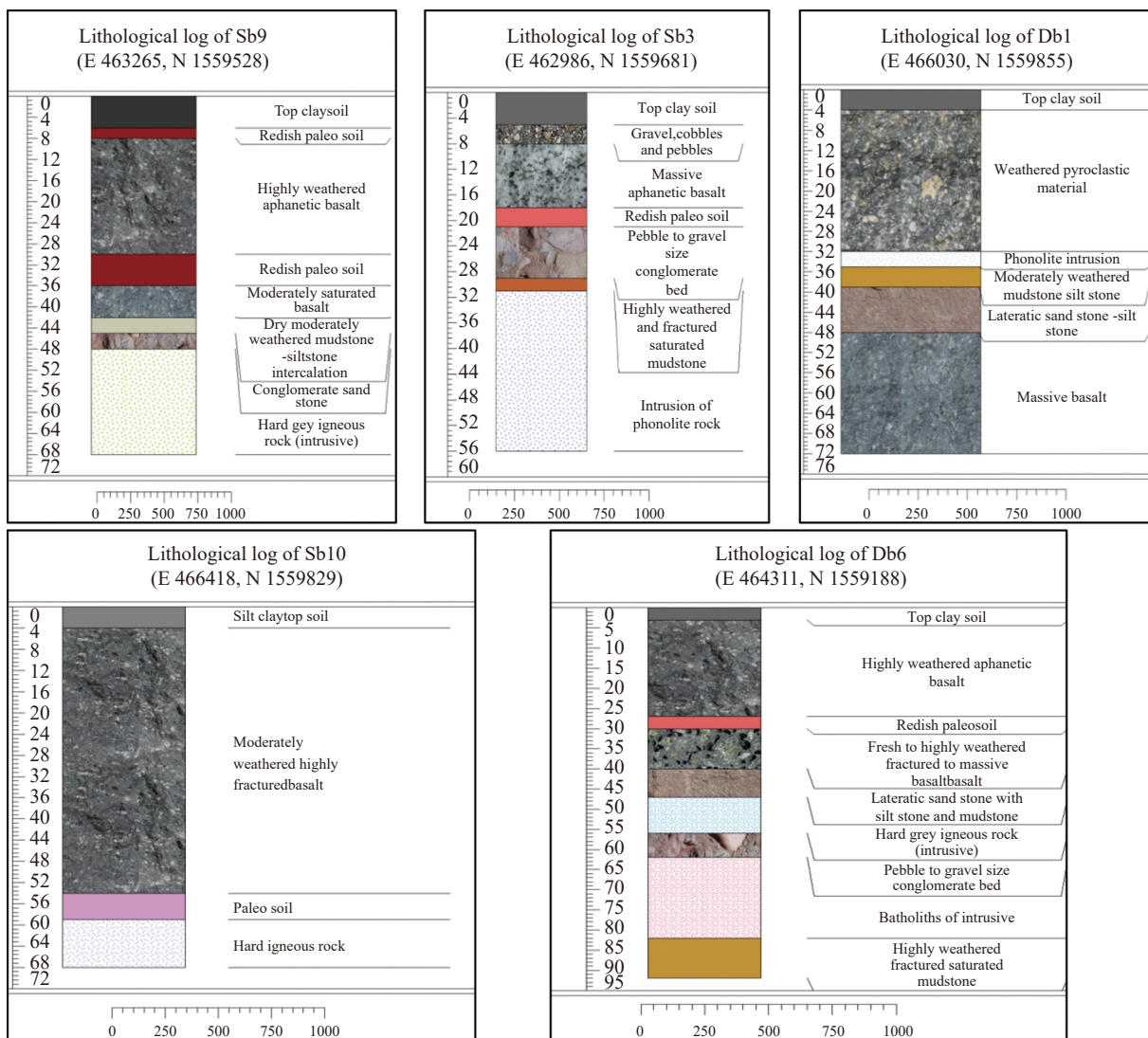


Fig. 6 Borehole log of selected areas with borehole samples (Sb9, Sb3, Db1, Sb10 and Db6)

validation to capture the horizontal and vertical variability in lithology, land use, geomorphology, and groundwater flow direction (Figs. 1, 2, and 3). Lithological boundaries were mapped and verified through field observations. Land cover and elevation data were derived from 30 m resolution satellite imagery and Digital Elevation Models (DEMs), respectively. Sampling sites were distributed across major lithological units and elevation gradients, and were positioned along upstream, midstream, and downstream sections of groundwater flow paths.

A total of 25 groundwater samples were collected from boreholes with depths ranging from 40 m to 150 m below the surface using APHA (2011) standard methods. The guidelines were adhered to for water sampling, transportation, storage, and analysis. A purposive sampling method was employed to obtain representative water samples across the study area (Kurniawan et al. 2023), ensuring comprehensive spatial coverage of key irrigation water sources at an approximate density of one sample per 10 km<sup>2</sup>. This sampling density is consistent with previous hydrogeochemical studies in similar semi-arid and geologically diverse regions and was considered adequate for capturing the representative spatial variability of groundwater quality in the study area.

Sampling was conducted during the dry season in March 2023 to reduce the influence of recent rainfall and surface runoff, thus providing more stable and representative groundwater quality data. Dry season sampling is commonly adopted in groundwater assessments within semi-arid regions like Northern Ethiopia, as it reflects baseline hydrochemical conditions with minimal dilution effects (Tegenge et al. 2023; Gintamo et al. 2022).

Before sampling, data sorting was conducted to ensure representativeness. Two categories of groundwater were considered: Functional boreholes located near agricultural lands and used as irrigation water sources, and non-functional boreholes deemed unsuitable for drinking due to water quality concerns but adapted for irrigation purposes. The criteria for sampling design also drew on previous research (e.g., Berhanu et al. 2023), which highlights the influence of geological formations, land use practices (such as agricultural runoff), and hydrological flow paths on water quality parameters, including mineral composition, nutrient levels, and pollutant concentrations. This varied sampling strategy was essential to capture the diversity of water quality influenced by both natural and anthropogenic factors, particularly

within agricultural environments.

To clean the well, the water was pumped for an average of 10 minutes before sampling (Zhu et al. 2019). Pre-cleaned 1,000 mL double cap high-density polyethylene (HDPE) storage bottles for anions and 500 mL storage bottles for cations and heavy metals were used. These bottles were cleaned with diluted HNO<sub>3</sub> and then rinsed with distilled water. Finally, they were washed three times with the sample solution prior to sample collection. After filtering all samples with 0.45 μm syringe filters, the samples were preserved with HNO<sub>3</sub> solution for cation analysis. No acidification of the samples was performed for anion analysis.

The HDPE sample containers were stored in a cooler, adequately labeled for identification, and transported to the laboratory for analysis. Electrical conductivity, Total Dissolved Solids (TDS), temperature, and pH were measured on-site using a portable pH meter, model HANNA HI9913. The probe used during measurements was rinsed with distilled water after each measurement to prevent cross-contamination between samples.

## 2.2 Laboratory analysis

The physicochemical parameters and heavy metals were analyzed using the analytical procedure prescribed in APHA (2017). The analysis took place in the geochemistry laboratory of Mekelle University. The cations and heavy metals such as Na<sup>+</sup>, Ca<sup>2+</sup>, K<sup>+</sup>, Mg<sup>2+</sup>, Fe, Zn, As, Ni, Pb, Cr, and Cu were examined using the Atomic Absorption Spectrometer (AAS). Meanwhile, anions such as Cl<sup>-</sup> and SO<sub>4</sub><sup>2-</sup> were examined using the UV spectrophotometer, with the reaction times and analytical reagents following the manufacturer's operating guidelines. The total hardness was determined using the EDTA titration method. The analysis of bicarbonate was carried out by titration using methyl orange as an indicator and 0.1 N hydrochloric acid as a titrant. To verify the analytical error during the analysis, the calculation of ionic charge balance error was applied using Equation 1 (Appelo and Postma, 2004). Almost all water samples showed an acceptable charge balance, usually with a limit of ±5%.

$$\text{Electron neutrality (\%)} = \frac{\sum \text{cation} - \sum \text{anion}}{\sum \text{cation} + \sum \text{anion}} \times 100 \quad (1)$$

Standard solutions were used to pre-calibrate the equipment used for each analysis, following inter-

national quality control and quality assurance (QC/QA) protocols. Before every measurement in both lab and field settings, all electrodes were meticulously cleaned with distilled water and sample solution. The correct stabilization time was ensured by conditioning the probes in the sample before each use. To prevent cross-contamination, sterile latex gloves and lab coats were worn when handling samples. To verify the precision of the measurements, a blank solution was utilized in addition to the standard solutions used for instrument calibration. Additionally, all AAS measurements were performed in triplicate and reported as mean values. The laboratory results provided the quantitative basis for subsequent statistical, graphical, and spatial analyses, which were used to derive the hydrochemical patterns and irrigation water quality indicators for the study area.

### 2.3 Data analysis and processing

Software such as ArcGIS 10.7, Aquachem 4.1, and the Statistical Package for Social Sciences (SPSS) version 20 were used to process and analyze the data collected. Inverse Distance Weighted (IDW) interpolation was utilized to create the spatial distribution maps of chemical indices. The processed dataset enabled a consistent comparison of groundwater chemistry across wells and physiographic zones. On this basis, a set of irrigation water quality parameters and indices was calculated to assess groundwater suitability for agricultural use.

### 2.4 Irrigation water quality parameters and indices

As summarized in Table 1, commonly used irrigation suitability parameters and indices, namely salinity hazard (EC), Total Dissolved Solids (TDS), Total Hardness (TH), Sodium Adsorption Ratio (SAR), Residual Sodium Carbonate (RSC), sodium percentage (Na%), Permeability Index (PI), Magnesium Ratio (MR), Kelly's Index (KI), and Potential Salinity (PS) were computed and classified according to published threshold values. Although individual parameters and indices provide valuable insights into specific constraints affecting irrigation suitability, an integrated assessment is required to capture their combined effects. Therefore, the Irrigation Water Quality Index (IWQI) was applied to evaluate and classify groundwater suitability using a single composite indicator.

### 2.5 Irrigation Water Quality Index (IWQI)

After Meireles et al. (2010), in addition to the individual water quality parameters and indices, an Irrigation Water Quality Index (IWQI) was computed. In the first step,  $Q_i$  was estimated using the following formula, which was developed by Ayers and Westcot (1985). According to the five more sensitive irrigation parameters, EC, SAR,  $\text{Na}^+$ ,  $\text{Cl}^-$ , and  $\text{HCO}_3^-$ , higher  $Q_i$  values indicate better suitability for irrigation.  $Q_i$  values are dimensionless.

$$Q_i = Q_{imax} - \left[ \frac{X_{ij} - X_{inf}}{X_{amp}} \right] \times Q_{iamp} \quad (2)$$

Where:  $Q_i$  is a quality-measuring value.  $Q_{imax}$  is the maximum  $Q_i$  value of the assigned quality class.  $X_{inf}$  represents the minimum threshold value of the category assigned to each parameter, and  $X_{ij}$  is the observed concentration value of the chemical parameters.  $Q_{iamp}$  is the class amplitude, and  $X_{amp}$  is the maximum value of the final class for each parameter.

As per Meireles et al. (2010), after calculating  $Q_i$ , accumulation weights ( $w_i$ ) were estimated such that the total cumulative weight equals 1, based on the guideline described in Table 2. Subsequently, the classification of irrigation water quality using the IWQI was carried out according to the criteria presented in Table 3.

The relative importance of each parameter used in the IWQI was determined based on its influence on irrigation water quality, particularly its impact on soil permeability, salinity, and plant toxicity, as established by Meireles et al. (2010) and Ayers and Westcot (1985). Parameters such as Electrical Conductivity (EC) and Sodium Adsorption Ratio (SAR) are known to exert strong control on soil structure and salinity hazards, while bicarbonate ( $\text{HCO}_3^-$ ), chloride ( $\text{Cl}^-$ ), and sodium ( $\text{Na}^+$ ) contribute to toxicity and sodicity risks.

Initial importance weights ( $w_i$ ) were assigned based on expert judgment and established literature, reflecting the relative criticality of each parameter for irrigation suitability. These initial values were then normalized to ensure their sum equals 1, using the following formula:

$$W_i = \frac{w'_i}{\sum_{i=1}^n w'_i} \quad (3)$$

Where:  $w'_i$  represents the raw importance, value assigned to parameter  $i$ , and  $n$  is the total number of parameters (in this case,  $n=5$ ). For this study,

**Table 1** Parameters, equations, and irrigation suitability classes used in the study area

Parameters	Equations	Range	Classification	References
EC (μS/cm)		<250	Excellent	Richards (1954)
		250–750	Good	
		750–2,250	Permissible	
		2,250–4,000	Doubtful	
TDS (mg/L)		<1,000	Non-saline	Robinove et al. (1958)
		1,000–3,000	Slightly saline	
		3,000–10,000	Moderately saline	
		>10,000	Very saline	
TH (mg/L)		<75	Soft	Vasanthavigar (2013)
		75–150	Moderate	
		150–300	Hard	
		>300	Very hard	
SAR (meq/L)	$(Na^+)/\sqrt{[(Ca^{2+} + Mg^{2+})/2]}$	<10	Excellent	Richards (1954)
		10–18	Good	
		18–26	Doubtful	
		>26	Unsuitable	
RSC (meq/L)	$(HCO_3^- + CO_3^{2-}) - (Ca^{2+} + Mg^{2+})$	<1.25	Good	Richards (1954)
		1.25–2.5	Medium	
		>2.5	Unsuitable	
Na%	$[(Na^+ + K^+)/ (Ca^{2+} + Mg^{2+} + K^+ + Na^+)] \times 100$	<20	Excellent	Wilcox (1955)
		20–40	Good	
		40–60	Permissible	
		60–80	Doubtful	
		>80	Unsuitable	
KI (meq/L)	$[(Na^+)/ (Ca^{2+} + Mg^{2+})]$	<1	Suitable	Kelly (1963)
		>1	Unsuitable	
PI%	$\left[ \left[ Na^+ + \sqrt{HCO_3^-} \right] / (Ca^{2+} + Mg^{2+} + Na^+) \right] \times 100$	<25	Unsuitable	Doneen (1975)
		25–75	Moderate	
		>75	Suitable	
MR%	$[(Mg^{2+}) / (Ca^{2+} + Mg^{2+})] \times 100$	<50	Suitable	Paliwal (1976)
		>50	Unsuitable	
PS (meq/L)	$Cl^- + \frac{1}{2}SO_4^{2-}$	<5	Excellent to good	Doneen (1975)
		5–10	Good to injurious	
		>10	Injurious to un satisfactory	

**Table 2** Normalized weight ( $w_i$ ) for the IWQI calculation and the parameter threshold values for the quality measurement ( $Q_i$ ) calculation (Meireles et al. 2010; Ayers and Westcot, 1985)

$Q_i$	EC (dS/m)	SAR (meq/L) <sup>1/2</sup>	Na <sup>+</sup> (meq/L)	Cl <sup>-</sup> (meq/L)	HCO <sub>3</sub> <sup>-</sup> (meq/L)
85–100	0.20 ≤ EC < 0.75	2 ≤ SAR < 3	2 ≤ Na <sup>+</sup> < 3	1 ≤ Cl < 4	1 ≤ HCO <sub>3</sub> <sup>-</sup> < 1.5
60–85	0.75 ≤ EC < 1.50	3 ≤ SAR < 6	3 ≤ Na <sup>+</sup> < 6	4 ≤ Cl < 7	1.5 ≤ HCO <sub>3</sub> <sup>-</sup> < 4.5
35–60	1.50 ≤ EC < 3.00	6 ≤ SAR < 12	6 ≤ Na <sup>+</sup> < 9	7 ≤ Cl < 10	4.5 ≤ HCO <sub>3</sub> <sup>-</sup> < 8.5
0–35	EC < 0.2 or EC ≥ 3.00	SAR < 2 or SAR ≥ 12	Na <sup>+</sup> < 2 or Na <sup>+</sup> ≥ 9	Cl < 1 or Cl ≥ 10	HCO <sub>3</sub> <sup>-</sup> < 1 or HCO <sub>3</sub> <sup>-</sup> ≥ 8.5
<b>Weight (<math>w_i</math>)</b>	<b>0.211</b>	<b>0.189</b>	<b>0.204</b>	<b>0.194</b>	<b>0.202</b>

the normalized weights were calculated based on the normalized values proposed by Meireles et al.

(2010) and were verified to maintain internal consistency with previous irrigation water quality

**Table 3** Water quality index characteristics classification (Meireles et al. 2010)

IWQI	Restrictions on water use	Recommendation	
		Soil	Plant
85–100	No Restriction required (NR)	Can be used for the majority of soil types with low probability of causing salinity and sodicity risks, except for soils with extremely low permeability	No toxicity risk for most plants
70–85	Low Restriction required (LR)	It should be used in light-texture or moderate permeability soils; recommended to avoid its use in soils with high clay levels	Avoid salt-sensitive plants
55–70	Moderate Restriction required (MR)	May be used in moderate to high soil permeability values of soils	Plants with moderate tolerance to salts may be grown
40–55	High Restriction required (HR)	May be used in soils with high permeability	It can be used for plants with moderate to high salt tolerance
0–40	Severe Restriction required (SR)	Should be avoided its use for irrigation under normal conditions	Plants with a high tolerance to salt should be irrigated only, except water with extremely low levels of Na <sup>+</sup> , Cl <sup>-</sup> , and HCO <sub>3</sub> <sup>-</sup>

studies conducted in semi-arid regions.

Finally, the IWQI was determined using the following equation:

$$IWQI = \frac{\sum_{i=1}^n W_i Q_i}{\sum_{i=1}^n W_i} \quad (4)$$

Where:  $W_i Q_i$  represents the quality score of a single water quality parameter after normalization and weighting.

In addition to groundwater quality parameters, soil texture and composition were explicitly considered in evaluating irrigation suitability, because infiltration capacity and contaminant attenuation vary significantly across different soil types. The spatial distribution of soils (Fig. 3) was therefore integrated to supplement the interpretation of IWQI results, establishing a linkage between groundwater quality and site-specific soil characteristics.

In summary, the analytical procedures, data processing steps, and irrigation water quality indices outlined above provide a robust and integrated framework for evaluating groundwater suitability for irrigation in the Aksum area. This framework facilitated the interpretation of hydrogeochemical characteristics and subsequent assessment of irrigation water quality using the selected indices, including the IWQI.

### 3 Results and discussion

#### 3.1 Hydrogeochemical characteristics of groundwater

The descriptive statistics of physicochemical parameters and major ions are presented in

<http://gwse.iheg.org.cn>

**Table 4.** The pH of groundwater samples ranged from 7.2 to 8.2, with an average of 7.5, which falls within the acceptable range for irrigation purposes. The slightly alkaline nature of the groundwater suggests that its pH is primarily controlled by the dissolution of carbonate and silicate minerals, which contribute higher concentrations of bicarbonate. Such water is unlikely to adversely affect soil structure or crop growth under typical irrigation practices.

Calcium (Ca<sup>2+</sup>) is the dominant cation in the study area, followed by sodium (Na<sup>+</sup>) and magnesium (Mg<sup>2+</sup>). Concentrations range from 22 mg/L to 325 mg/L, with a mean of 86.8 mg/L (Table 4). In the absence of national guidelines, Ayres and Westcot (1985) recommend a permissible limit of 400 mg/L, and all samples fall within this range. Elevated calcium concentrations are observed in basaltic aquifers, mainly due to the dissolution of calcium-bearing silicate minerals (e.g., anorthite) facilitated by CO<sub>2</sub>, and locally from secondary carbonate minerals (calcite, dolomite) occurring as veins within basalt formations. Lower calcium concentrations in some wells may reflect cation exchange processes, where Ca<sup>2+</sup> is replaced by Na<sup>+</sup>. Calcium is essential for plant nutrition and soil structure, but both deficiency and excess can impair plant growth and soil permeability. Although the water meets quality standards, crop-specific sensitivity should be considered for sustainable irrigation practices.

Magnesium (Mg<sup>2+</sup>) concentrations range from 8 mg/L to 160 mg/L, with a mean of 43.5 mg/L. Higher values occur in basaltic aquifers, while lower concentrations are found in phonolite and trachyte aquifers. Deep wells generally show higher Mg<sup>2+</sup> than shallow ones. Although Ethiopia lacks national guidelines, Ayres and Westcot (1985) recommend a threshold above which 16%

**Table 4** Descriptive statistics of major ions and miscellaneous chemical parameters (unit=mg/L except pH)

Parameters	Min	Max	Mean	SD	Maximum allowable limit (Ayres and Westcot, 1985)	% above standard
pH	7.2	8.2	7.5	0.32	6–9	0
Ca <sup>2+</sup>	22	325	86.8	71.1	<400	0
Mg <sup>2+</sup>	8	160	43.5	34.1	<60	16
K <sup>+</sup>	0.6	22	3.79	5.59	<20	0
SO <sub>4</sub> <sup>2-</sup>	8.9	99	33.3	22.1	<960	0
Cl <sup>-</sup>	7.6	74	33.3	6.9	<106.5	0
NO <sub>3</sub> <sup>-</sup>	15.2	37.1	20.5	5.4	<30	32
NO <sub>2</sub> <sup>-</sup>	0.01	0.18	0.06	0.044	<1.6	0
HCO <sub>3</sub> <sup>-</sup>	103.7	433.1	280	98.6	<610	0
NH <sub>4</sub> <sup>+</sup>	0.12	0.45	0.21	0.09	<5	0
PO <sub>4</sub> <sup>3-</sup>	0.003	1.02	0.14	0.26	<2	0

of the samples exceed acceptable limits (Table 4). The similar trends of Ca<sup>2+</sup> and Mg<sup>2+</sup> indicate a common source, primarily basaltic lithology. While most samples meet the guideline, elevated magnesium in some areas may adversely affect soil structure and permeability. High Mg<sup>2+</sup>, especially when accompanied by low Ca<sup>2+</sup>, promotes soil dispersion, reducing infiltration and impairing crop growth. These findings highlight the importance of monitoring magnesium hazards in basalt-dominated hydrogeological settings.

Potassium (K<sup>+</sup>) concentrations range from 0.6 mg/L to 22 mg/L, with a mean of 3.79 mg/L (Table 4). All samples are within the permissible irrigation standard. Higher values are associated with alkaline basalt aquifers, showing spatial patterns similar to Ca<sup>2+</sup> and Na<sup>+</sup>. Although elevated potassium can interfere with nutrient uptake in plants (Swistock, 2016), the measured concentrations do not pose a risk to irrigation suitability.

Groundwater chemistry in the study area is primarily controlled by water-rock interactions. According to the Gibbs diagram, 81% of the samples plot within the rock-water interaction dominance field (Figs. 7a and 7b), indicating that mineral dissolution during groundwater flow from recharge to discharge zones is the main source of major ions.

The concentration of sulfate (SO<sub>4</sub><sup>2-</sup>) in the groundwater samples ranged from 8.9 mg/L to 99 mg/L, with an average of 33.6 mg/L (Table 4), making it the second most abundant anion after bicarbonate. The highest concentrations were recorded in deep wells, while the lowest levels were in shallow wells. Elevated sulfate concentrations in areas surrounding Aksum town and irrigation areas may be attributed to anthropogenic inputs such as fertilizer application and municipal

waste discharge. Despite these localized increases, all sulfate concentrations remain within the permissible limits for irrigation, indicating no immediate concern related to sulfate toxicity. The scatter plot in Fig. 7c shows a strong correlation between sulfate and chloride, confirming that anthropogenic activities are a major contributor to elevated sulfate concentrations near the town and agricultural areas.

The concentration of chloride (Cl<sup>-</sup>) ranged from 7.6 mg/L to 74 mg/L, with an average of 33.3 mg/L (Table 4). The highest value was detected in a deep well, while the lowest was in a shallow well. Elevated chloride levels, especially near Aksum town, suggest that urban waste, along with natural sources like volcanic activity, may contribute to the higher Cl<sup>-</sup> concentrations. The scatter diagrams in Figs. 7c and d, showing chloride against nitrate and sulfate, indicate the influence of anthropogenic activities on increasing chloride levels (Subramanian et al. 2010). However, all observed chloride levels remain within the permissible limits set by the FAO for irrigation.

The bicarbonate (HCO<sub>3</sub><sup>-</sup>) concentration ranged from 103.7 mg/L to 433.1 mg/L, with a mean value of 280 mg/L (Table 4). Bicarbonate is the dominant anion, followed by sulfate (SO<sub>4</sub><sup>2-</sup>) and chloride (Cl<sup>-</sup>). The highest concentrations were recorded in basaltic rock aquifers. The elevated bicarbonate concentrations are attributed to the dissolution of silicate and carbonate minerals, including calcite and dolomite, which occur as veins within the volcanic rocks. In addition, the interaction between dissolved CO<sub>2</sub> and alkaline volcanic lithology enhances bicarbonate levels through weathering processes (Alemayehu, 2011). All water sources remain within the acceptable

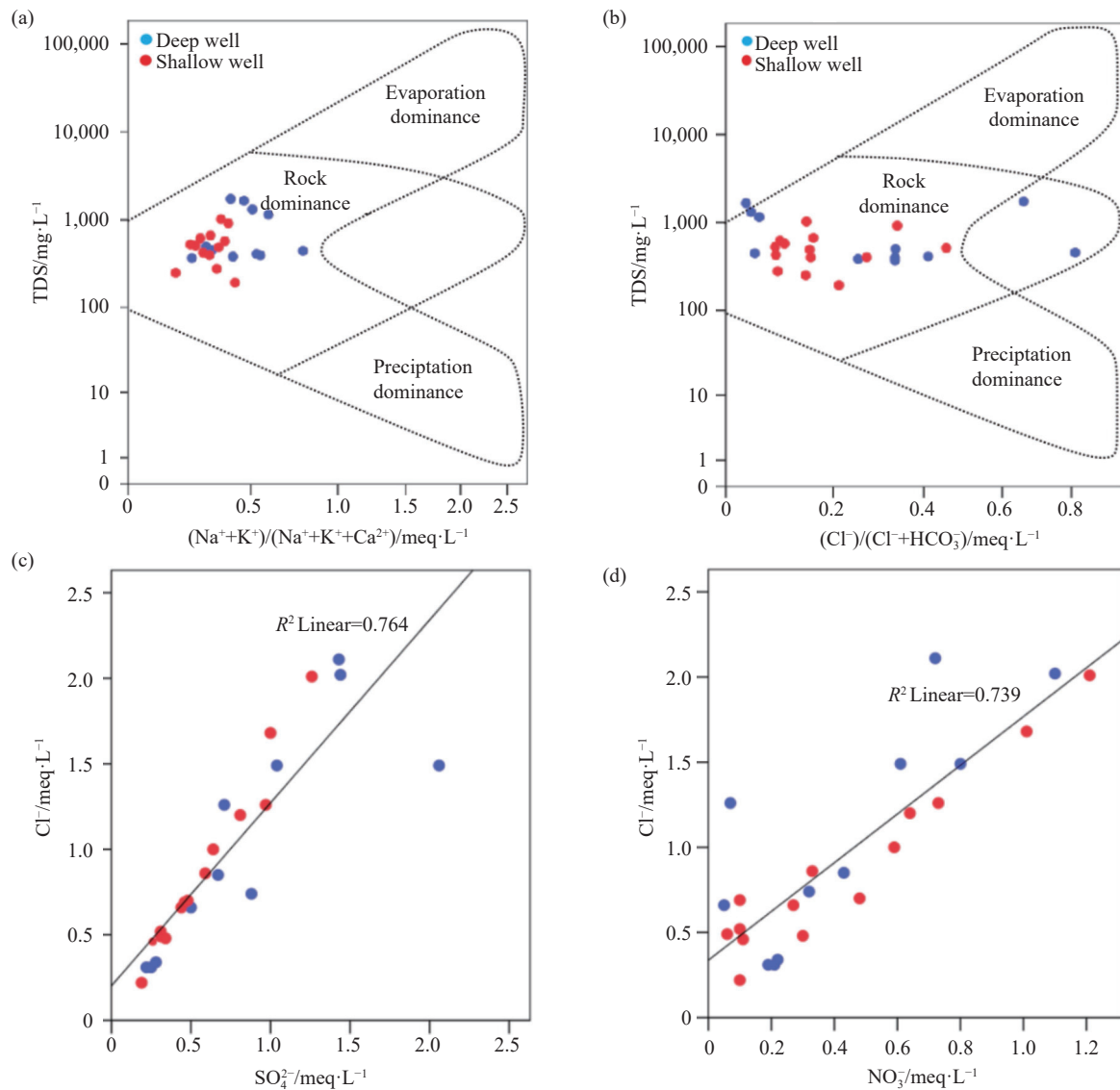


**Fig. 7** Diagrams illustrating the mechanisms controlling groundwater chemistry

(a, b) Gibbs diagrams showing the mechanisms controlling groundwater chemistry; (c) Scatter diagram of  $\text{Cl}^-$  against  $\text{SO}_4^{2-}$ ; (d) Scatter diagram of  $\text{Cl}^-$  against  $\text{NO}_3^-$ .

limits for irrigation (Table 4).

The concentration of nutrients in groundwater clearly shows human influence. Nitrate ( $\text{NO}_3^-$ ) levels ranged from 15.2 mg/L to 37.1 mg/L (average 20.5 mg/L), with 32% of the samples exceeding the permissible limit, especially in shallow wells near agricultural land and waste disposal sites (Table 4). Nitrite ( $\text{NO}_2^-$ ) varied from 0.01 mg/L to 0.18 mg/L (average 0.06 mg/L), while ammonium ( $\text{NH}_4^+$ ) ranged from 0.12 mg/L to 0.45 mg/L (average 0.21 mg/L). Both parameters exhibited their highest concentrations in shallow wells close to farms and urban areas, but remained within recommended safety limits. Phosphate ( $\text{PO}_4^{3-}$ ) ranged from 0.003 mg/L to 1.02 mg/L (average 0.14 mg/L), with higher values near farming zones and town outskirts, although all samples

remained below the permissible level (Table 4). Elevated nitrate concentrations are of particular concern because they exceed recommended standards and may contribute to excessive plant growth and potential crop toxicity (Ayres and Westcot, 1985). Although nitrite, ammonium, and phosphate concentrations were within acceptable limits, their spatial distribution indicates localized contamination from fertilizer application, agricultural runoff, and municipal waste seepage.

Overall, groundwater chemistry in the study area reflects the interplay of water-rock interactions and anthropogenic inputs, which collectively drive the accumulation of major ions and nutrients. These patterns highlight the importance of continued monitoring and management to protect soil quality, crop productivity, and environmental sustainabil-

ity. Given the potential risks posed by trace metals, the subsequent analysis focuses on evaluating heavy metal concentrations and their implications for irrigation suitability.

### 3.2 Heavy metal toxicity

Table 5 displays the heavy metal concentration in water samples from the study area. The distribution of heavy metals varies by elements, and the overall abundance follows the order: Fe > Zn > As > Ni > Pb > Cr > Cu (Fig. 8). Their concentration ranges are as follows: Fe (0.002–2.38 mg/L), Zn (0.001–0.6 mg/L), As (0.0001–0.064 mg/L), Ni (0.0012–0.06 mg/L), Pb (0.00001–0.016 mg/L), Cr (0.000003–0.012 mg/L), and Cu (0.0009–0.01 mg/L). These results indicate that all measured heavy metal concentrations fall within the recommended standards for irrigation use. Having established that heavy metals do not pose an immediate constraint, the analysis now focuses on conven-

tional irrigation water quality parameters and indices that more directly affect soil properties and crop performance.

### 3.3 Irrigation water quality parameters and indices

As per Wilcox's (1955) classification diagram for water samples based on salinity and sodium hazard, the samples fall into the medium, high, and very high salinity range (Figs. 9 and 10). Due to osmoregulation disruption, cell damage, salt buildup in root zones, and other factors, the saline nature of irrigation water in the study area can harm crops (El Bilali and Taleb, 2020). Higher salt concentrations also negatively affect soil fertility and structure, impede plant growth, reduce crop yields, and disrupt soil microbial communities (Tarolli et al. 2024; Zhou et al. 2024). Therefore, the observed salinity hazard levels highlight the pressing need for improved irrigation water qual-

**Table 5** Descriptive statistics and recommended maximum levels of heavy metal concentration in water used for irrigation

Parameters (mg/L)	Min.	Max.	Mean	Std.	Maximum limit (Ayers and Westcot, 1985)	Samples exceed Standard (%)
Fe	0.002	2.38	0.68	0.68	5	0
Cu	0.0009	0.01	0.0033	0.0025	0.2	0
Pb	0.00001	0.016	0.0027	0.0034	5	0
Cr	0.000003	0.012	0.0009	0.002	0.1	0
Zn	0.001	0.6	0.076	0.12	2	0
Ni	0.0012	0.06	0.035	0.374	0.2	0
As	0.0001	0.064	0.0039	0.013	0.1	0

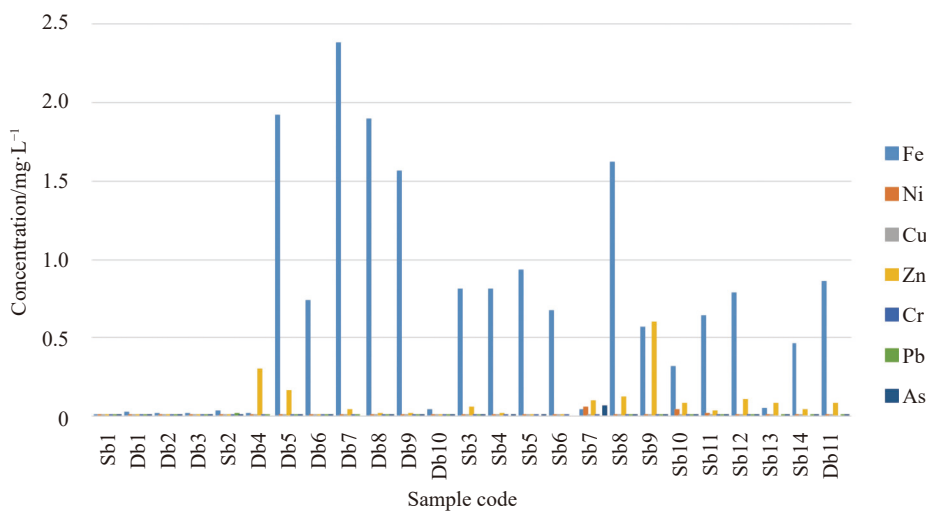


**Fig. 8** Concentrations of heavy metals in water samples

ity management and salinity control practices (Shitu et al. 2022).

The mean Total Dissolved Solids (TDS) concentration was 647.9 mg/L, ranging from 195.8 mg/L to 1,735 mg/L (Table 6). Based on the classification by Robinove et al. (1958), the samples vary from non-saline to slightly saline, with 80% falling in the non-saline category and 20% in the slightly saline category. Elevated soluble salts reduce the

availability of soil moisture to crops, even under adequate soil water conditions, thereby limiting plant water uptake (Berhe, 2020; Masoud et al. 2022). The presence of slightly saline water suggests that continued irrigation could gradually lead to soil salinization and reduced agricultural productivity (Gebrehiwot et al. 2021; Shitu et al. 2022).

Higher EC and TDS values were recorded in the

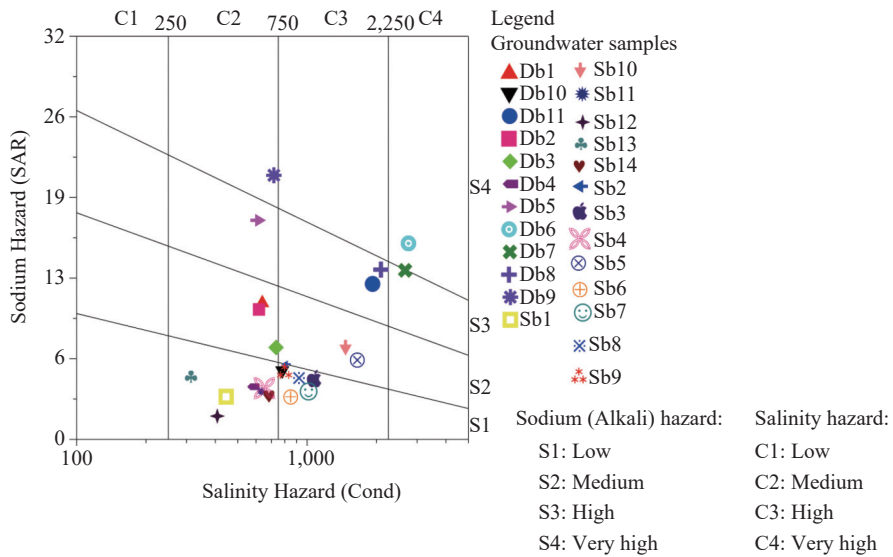
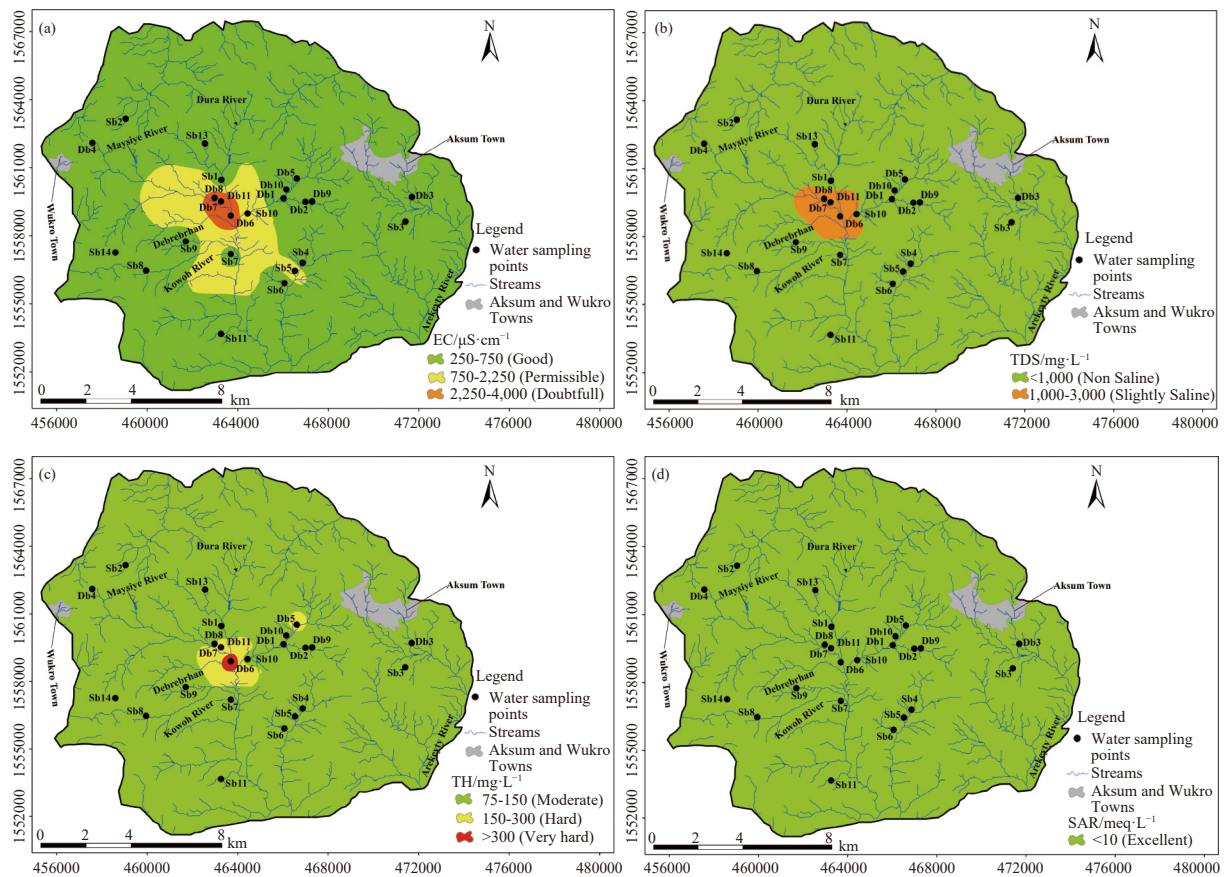
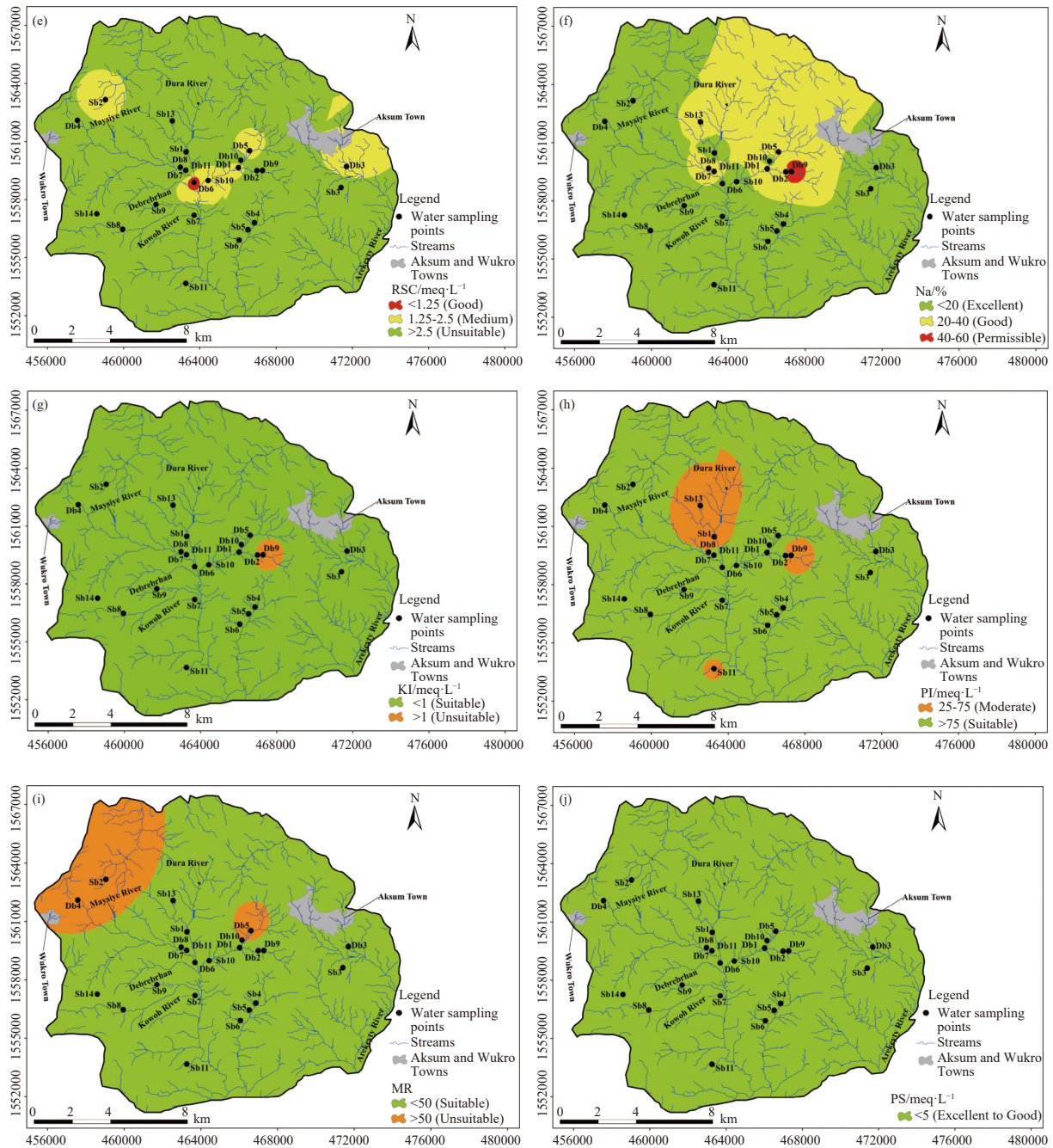


Fig. 9 Classification of water samples based on salinity (EC) and sodium hazard (according to Wilcox, 1955)





**Fig. 10** Spatial distribution of irrigation water quality parameters in the study area

Notes: Including electrical conductivity (EC), total dissolved solids (TDS), total hardness (TH), sodium adsorption ratio (SAR), residual sodium carbonate (RSC), sodium percentage (Na%), Kelly index (KI), permeability index (PI), magnesium ratio (MR), and potential salinity (PS). The corresponding classification criteria and suitability classes are indicated in the legend.

central part of the study area near Debrebrhan and Kowah Rivers, coinciding with zones of elevated salinity hazard (Fig. 10). This pattern is primarily attributed to the dissolution of calcite- and dolomite-bearing veins within extensively weathered basaltic rocks. The central area's lower elevation and convergence of multiple streams further promote the accumulation and concentration of dissolved salts. In addition, faults and fractures enhance water-rock interaction, thereby accelerat-

ing mineral dissolution and the transport of ions.

Total Hardness (TH) in the study area ranged from 87.9 mg/L to 1,470.5 mg/L, with an average of 395.8 mg/L (Table 6). According to Vasanthavigar's (2013) classification, the water samples range from moderately hard to very hard. The majority of the samples (60%) fell within the very hard category, while 32% were classified as hard and the remaining 8% as moderate. The high hardness, especially in the central part of the study area (Fig.

**Table 6** Descriptive statistics of irrigation water quality parameters and the calculated indices

Parameters	Sample range				Standard Range	Classification	% of samples with standard
	Min.	Max.	Mean	Std.			
EC ( $\mu\text{S}/\text{cm}$ )	306	2,711	1,012.4	647	<250	Excellent	0
					250–750	Good	48
					750–2,250	Permissible	40
					2,250–4,000	Doubtful	12
TDS ( $\text{mg}/\text{L}$ )	195.8	1,735	647.9	414.1	<1,000	Non saline	80
					1,000–3,000	Slightly saline	20
					3,000–10,000	Moderately saline	0
					>10,000	Very saline	0
TH ( $\text{mg}/\text{L}$ )	87.9	1,470.5	395.8	275	<75	Soft	0
					75–150	Moderate	8
					150–300	Hard	32
					>300	Very hard	60
SAR ( $\text{meq}/\text{L}$ )	0.28	3.51	1.33	0.88	<10	Excellent	100
					10–18	Good	0
					18–26	Doubtful	0
					>26	Unsuitable	0
RSC ( $\text{meq}/\text{L}$ )	–28.3	9.3	–2	6.95	<1.25	Good	80
					1.25–2.5	Medium	4
					>2.5	Unsuitable	16
Na%	10.5	57.8	24.8	10	<20	Excellent	40
					20–40	Good	56
					40–60	Permissible	4
					60–80	Doubtful	0
					>80	Unsuitable	0
KI ( $\text{meq}/\text{L}$ )	0.11	1.34	0.35	0.24	<1	Suitable	96
					>1	Unsuitable	4
PI%	28	89	50.6	15.6	<25	Unsuitable	0
					25–75	Moderate	12
					>75	Suitable	88
MR%	8.6	71	46	13.7	<50	Suitable	68
					>50	Unsuitable	32
PS ( $\text{meq}/\text{L}$ )	0.31	2.8	1.3	0.77	<5	Excellent to good	100
					5–10	Good to injurious	0
					>10	Injurious to Un satisfactory	0

10), is mainly due to the dissolution of carbonate minerals such as calcite within volcanic rock veins. In addition, weathering of silicate-rich volcanic rocks (e.g., basalt, rhyolite) releases calcium, magnesium, sodium, and bicarbonate ions, which increase water hardness. Similar processes have been observed in the Golina River Basin (Gebbru et al. 2024), the Konso volcanic terrain (Abebe et al. 2024), and the Dawa River Basin (Woldemariam and Ayenew, 2016). Additionally, during the dry season, reduced recharge and intense evaporation

concentrate dissolved ions, further raising water hardness. These findings are consistent with regional hydrogeochemical patterns in Ethiopia, where volcanic terrains usually produce harder and more alkaline waters compared to sedimentary or alluvial regions. For example, groundwater in alluvial deposits of Laelay Maichew shows lower hardness and salinity, providing better conditions for irrigation (Gebrehiwot et al. 2021). In contrast, Aksum's volcanic environment and semi-arid climate create a hydrogeochemical setting where

water quality issues are more significant (Habtu et al. 2020).

The Sodium Adsorption Ratio (SAR) in the study area ranged from 0.28 meq/L to 3.51 meq/L, with a mean of 1.33 meq/L. According to Richards' (1954) classification, all samples fall within the excellent category for irrigation suitability (Table 6). The spatial distribution (Fig. 10) confirms that SAR values are uniformly low across the study area. Although SAR values are within safe limits, elevated sodium in soils can replace calcium and magnesium, causing soil deflocculation. This process reduces infiltration and permeability, restricts nutrient and water availability, and ultimately lowers crop productivity (Gaikwad et al. 2020). Sodic soils are further characterized by dispersed clay particles and fine pore dominance, which hinder water movement and weaken soil structure (Zhou et al. 2024).

Residual Sodium Carbonate (RSC) is a crucial parameter for evaluating irrigation water quality, as it indicates the equilibrium between  $\text{CO}_3^{2-}/\text{HCO}_3^-$  and  $\text{Ca}^{2+}/\text{Mg}^{2+}$ . Elevated carbonate and bicarbonate levels precipitate  $\text{Ca}^{2+}$  and  $\text{Mg}^{2+}$ , increasing soil sodicity by enhancing sodium adsorption (Richards, 1954; Hedjal et al. 2018). Richards (1954) classifies irrigation water as good ( $\text{RSC} < 1.25$ ), moderately suitable ( $1.25-2.5$ ), or unsuitable ( $\text{RSC} > 2.5$ ). In the study area, RSC values ranged from  $-28.3$  meq/L to  $9.3$  meq/L, with a mean of  $-2$  meq/L. About 80% of the samples are classified as good, 4% as moderately suitable, and 16% as unsuitable (Table 6). Higher RSC values occur in the central part of the study area, near Debrebrhan and Kowoh Rivers, coinciding with zones dominated by weathered alkaline basalt (Fig. 10). Here, bicarbonate ions react with  $\text{Ca}^{2+}$  and  $\text{Mg}^{2+}$ , reducing their free concentrations and increasing sodium levels, primarily as sodium carbonate, which drives positive RSC values. Elevated RSC not only degrades soil quality but can also cause corrosion in irrigation system components such as emitters (Kumari et al. 2022).

Sodium is a key parameter in classifying irrigation water because it influences soil permeability through interactions with clay and humus particles (Mukiza et al. 2021). In the study area, Na% ranged from 10.5% to 57.8%, with a mean of 24.8% (Table 6). The spatial distribution map (Fig. 10) shows that most of the area has low Na% values, with the majority of samples falling within the excellent to good categories. However, a few samples with elevated sodium, as indicated near the Town of Aksum in areas dominated by phonolite and trachyte rocks, can pose risks of soil degra-

dition by dispersing clay and humus, which clog macropores, reduce infiltration and percolation, and limit water availability to crops (El Osta et al. 2022; Gad et al. 2021). According to Wilcox's (1955) classification, over 70% of the samples fall within the good to permissible category, approximately 24% in the excellent to good range, and two samples are classified as doubtful to unsuitable (Fig. 11).

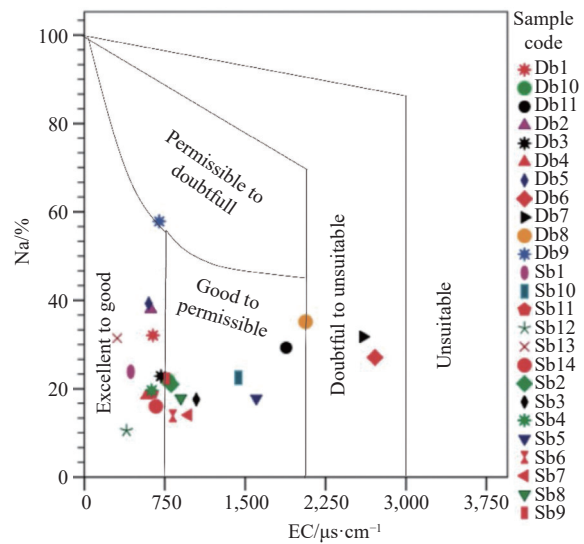
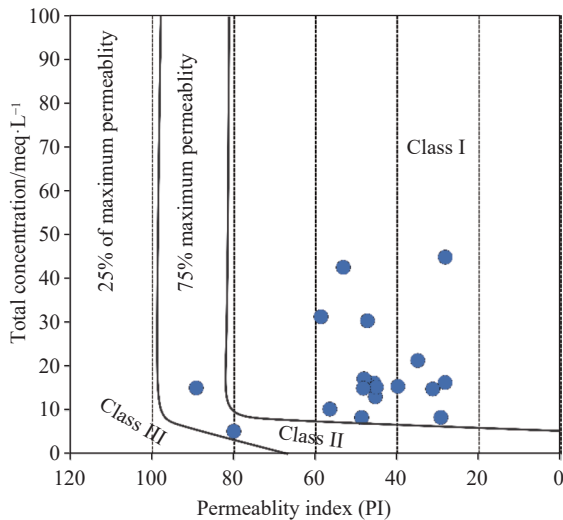


Fig. 11 Wilcox's (1955) diagram showing the relation between sodium percent and salinity hazard (EC)

The computed Kelly Index (KI) values ranged from 0.11 meq/L to 1.34 meq/L, with an average of 0.35 meq/L. Based on the KI evaluation, 96% of the water sources are suitable for irrigation, while only one sample is unsuitable (Table 6). The spatial distribution map (Fig. 10) further shows that more than 90% of the area is covered by water classified as excellent for irrigation.

Long-term use of saline irrigation water can affect soil permeability due to the influence of  $\text{HCO}_3^-$ ,  $\text{Ca}^{2+}$ ,  $\text{Mg}^{2+}$ , and  $\text{Na}^+$  concentrations (Vasanthavigar et al. 2013). Doneen (1975) proposed the Permeability Index (PI) for evaluating water suitability for irrigation. In the study area, PI values range from 28% to 89%, with an average of 50.6%. The spatial distribution map (Fig. 10) indicates that more than 70% of the study area are covered by water classified as suitable for irrigation purposes. In addition to the spatial distribution map, the Doneen diagram further verifies. About 88% of the samples fall into Class I ( $\text{PI} > 75\%$ ), representing suitable water quality, while 12% fall into Class II ( $\text{PI} = 25-75\%$ ), indicating moderate water quality (Table 6, and Fig. 12).

The Magnesium Ratio (MR) values ranged from 8.6% to 71%, with a mean of 46% (Table 6).



**Fig. 12** Doneen diagram of permeability index against the total concentration of ions (Doneen, 1975)

Based on Paliwal's (1976) classification, 68% of the groundwater samples are suitable for irrigation, while 32% are unsuitable. The spatial distribution map (Fig. 10) shows that most of the study area is covered by suitable water, with only a limited zone near Mysiyee River, falling into the unsuitable category.

The calculated Potential Salinity (PS) values ranged from 0.31 meq/L to 2.8 meq/L, with a mean of 1.3 meq/L. According to Doneen's (1975) classification, all water samples fall within the excellent to good category for irrigation use (Table 6). The spatial distribution map (Fig. 10) further confirms that the entire study area is suitable for irrigation with respect to PS.

Taken together, these individual parameters and indices offer a detailed, though fragmented, assessment of groundwater suitability for irrigation. To synthesize their combined effects into a unified, spatially explicit evaluation, the study applies the Irrigation Water Quality Index (IWQI) across the study area.

### 3.4 Irrigation Water Quality Index (IWQI)

The Irrigation Water Quality Index (IWQI) is a useful tool for assessing the suitability of water sources for irrigation because it offers a clear classification of plant toxicity and soil impacts (Masoud et al. 2022; Bennet, 2023). The evaluation of water suitability for irrigation was frequently based on individual parameters like SAR, EC, RSC, KI, Na%, MR, PS, and PI. However, by integrating combined indices, it is possible to significantly improve the assessment framework and provide more thorough and actionable insights,

which is highly advantageous for decision-makers (Gad et al. 2021). According to Ayers and Westcott (1985) and Adimalla et al. (2020), five different hazard groups were used to assess the suitability of groundwater for irrigation. This method offers a more thorough understanding of the safety and quality of water by integrating multiple parameters, including EC, SAR,  $\text{Na}^+$ ,  $\text{Cl}^-$ , and  $\text{HCO}_3^-$ , into a single evaluation framework. This approach is particularly valuable because it takes into account a variety of variables that impact crop health, irrigation effectiveness, and overall agricultural production. It also offers a thorough picture of water quality, which makes it simpler to spot general patterns and rank interventions. It offers vital information for accurately assessing the quality of irrigation water in areas with similar hydrogeological and environmental characteristics. It also encourages the sustainable management of water resources and is a versatile instrument that can be applied in a variety of geographical locations and environmental conditions around the world.

According to the Irrigation Water Quality Index (IWQI) classification proposed by Meireles et al. (2010), there are five categories: No restriction, low restriction, moderate restriction, high restriction, and severe restriction. In the present study, 36% of the water samples fell into the high restriction class, indicating that this water can be applied only to soils with high permeability and for crops with moderate to high salt tolerance (Table 7). About 32% of the samples are also classified as water that requires moderate restriction, suggesting that this water can be used in soils with moderate to high permeability and for plants with moderate to high salt tolerance. A further 24% of the samples fell within the severe restriction category, implying that such water should generally be avoided for irrigation under normal conditions; it should only be used to irrigate salt-tolerant crops, and preferably where  $\text{Na}^+$ ,  $\text{Cl}^-$ , and  $\text{HCO}_3^-$  concentrations are relatively low (Meireles et al. 2010). Only 8% of the water samples fell into the low-restriction class. This type of water is recommended for use in soils with moderate permeability and light texture and should be avoided in areas with high clay content and for salt-sensitive plants (Meireles et al. 2010).

The spatial distribution of IWQI classes (Fig. 13a) shows that the water samples taken from the south-western and parts of the western portion are dominated by water requiring severe restriction, whereas the water from the southern, central, and parts of the northern area is predominantly charac-

**Table 7** Irrigation water quality index results of water samples

Sample points	W <sub>i</sub> Q <sub>i</sub> (EC)	W <sub>i</sub> Q <sub>i</sub> (SAR)	W <sub>i</sub> Q <sub>i</sub> (Na <sup>+</sup> )	W <sub>i</sub> Q <sub>i</sub> (Cl)	W <sub>i</sub> Q <sub>i</sub> (HCO <sub>3</sub> <sup>-</sup> )	ΣW <sub>i</sub> Q <sub>i</sub>	ΣW <sub>i</sub>	IWQI
Sb1	19.8	3.3	3.6	3.4	16.0	46.1	1	46.1
Db1	18.6	3.3	15.9	3.4	18.9	60.0	1	60.0
Db2	18.7	3.3	18.4	3.4	3.5	47.3	1	47.3
Db3	18.1	3.3	18.0	18.4	3.5	61.3	1	61.3
Sb2	17.5	3.3	19.3	19.2	17.5	76.9	1	76.9
Db4	18.9	3.3	3.6	3.4	3.5	32.7	1	32.7
Db5	18.8	15.6	7.5	18.9	12.2	73.1	1	73.1
Db6	8.4	16.9	3.6	18.9	3.5	51.3	1	51.3
Db7	8.8	18.0	12.0	3.4	3.5	45.7	1	45.7
Db8	10.7	18.0	13.5	3.4	3.5	49.1	1	49.1
Db9	18.2	15.3	14.7	3.4	9.7	61.3	1	61.3
Db10	17.7	3.3	3.6	18.3	12.6	55.5	1	55.5
Sb3	15.9	3.3	3.6	19.2	9.5	51.4	1	51.4
Sb4	18.6	3.3	3.6	3.4	13.3	42.2	1	42.2
Sb5	12.3	3.3	19.1	19.4	10.5	64.5	1	64.5
Sb6	17.4	3.3	3.6	3.4	11.3	39.0	1	39.0
Sb7	16.4	3.3	3.6	3.4	10.0	36.6	1	36.6
Sb8	16.9	3.3	3.6	3.4	10.4	37.5	1	37.5
Sb9	17.8	3.3	3.6	3.4	11.8	39.9	1	39.9
Sb10	13.1	3.3	18.5	18.4	13.1	66.4	1	66.4
Sb11	18.6	3.3	3.6	18.7	12.1	56.3	1	56.3
Sb12	20.0	3.3	3.6	3.4	14.9	45.2	1	45.2
Sb13	20.5	3.3	3.6	3.4	16.8	47.6	1	47.6
Sb14	18.4	3.3	3.6	3.4	11.1	39.7	1	39.7
Db11	11.3	18.9	14.2	19.2	3.5	67.1	1	67.1

terized by high-restriction water. These patterns are likely associated with intensive agricultural activities and wastewater or solid waste inputs from nearby settlements, which can enhance salinity and sodicity, thereby deteriorating irrigation water quality.

The association between soil distribution and IWQI results revealed distinct spatial patterns of irrigation suitability (Fig. 13b). Areas dominated

by sandy clay loam, silty clay loam, and clay soils largely correspond to zones where irrigation water falls into the high to severe restriction classes, indicating that soils with lower permeability can exacerbate salinity and sodicity problems by limiting leaching. In particular, silty clay loam soils frequently coincide with IWQI zones classified as having high restriction, reflecting reduced leaching capacity and greater vulnerability to salinity

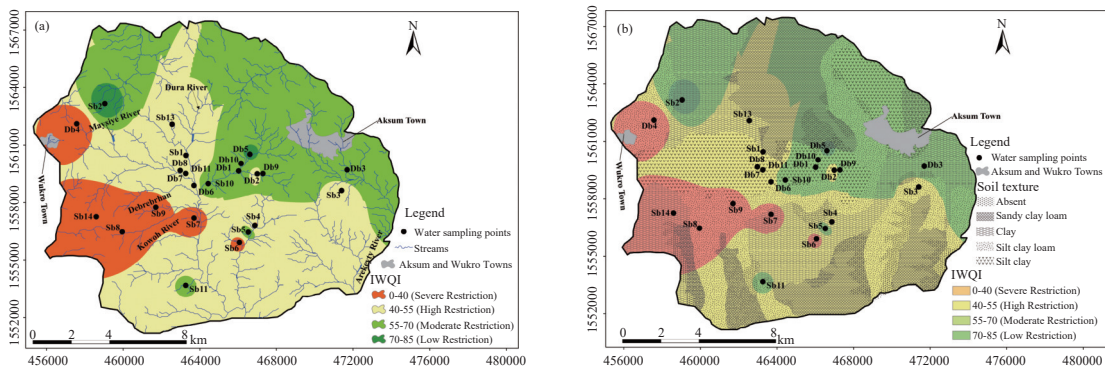


**Fig. 13** Spatial distribution of the Irrigation Water Quality Index (IWQI) in the study area

(a) Spatial distribution of IWQI in relation to physiographic characteristics; (b) Spatial distribution of IWQI in relation to soil texture classes.

buildup. Areas with silty clay and silty clay loam also commonly align with high restriction categories, suggesting that, in these locations, the combination of soil texture and water quality is not favorable for long-term irrigation without careful management. Conversely, some clay-dominated areas in the central and western parts of the study area coincide with zones classified as having low restriction, whereas other clay areas are associated with moderate or high restrictions. This spatial variability indicates that, although clay soils generally have low permeability and limited infiltration, they can still retain sufficient water for plant use, and their irrigation suitability is strongly dependent on local water quality. Overall, integrating IWQI with soil texture data demonstrates that soil properties exert a strong control on the spatial variability of irrigation suitability in the Aksum area and emphasizes the need to jointly consider both water quality and soil characteristics in irrigation planning and management.

The relationship between the IWQI and physiography in the Aksum area was non-uniform. Although high IWQI values (high and severe restriction) are commonly expected in discharge zones and low-lying landscapes, the observed patterns are more complex. Both high and low IWQI classes occurred in low-lying areas, and some recharge zones also exhibited high IWQI. In low-lying areas where the IWQI is high, intensive irrigated agriculture and proximity to settlements likely promote salt accumulation through irrigation return flow, fertilizer leaching, and domestic waste inputs, leading to elevated EC,  $\text{Na}^+$ ,  $\text{Cl}^-$ , and SAR. In contrast, low-lying zones with low to moderate IWQI are mostly associated with less intensive land use and appear to receive relatively fresh recharge from upstream lithologies with lower salinity, which limits salt buildup.

In several topographic recharge areas, high IWQI values corresponded with outcrops of fine-grained saline igneous and sedimentary units and intensively cultivated land. Infiltrating water in these zones may rapidly dissolve salts from geological materials and incorporate agrochemical inputs, resulting in local salinization and sodification of shallow groundwater. These findings indicate that in the Aksum area, lithological and land use locally control irrigation water quality.

The IWQI results, together with their relationships to soil conditions and physiographic factors, provide an integrated appraisal of groundwater suitability for irrigation in the study area. These findings form the basis for the subsequent conclusions and implications for sustainable groundwa-

ter use and irrigation management in the Aksum area.

## 4 Conclusion

This study provided a comprehensive evaluation of irrigation water quality in the semi-arid area of Aksum, Northern Ethiopia, by applying the Irrigation Water Quality Index (IWQI) integrated with GIS. The results indicate that most of the groundwater sources are suitable for irrigation, but some parameters, such as magnesium, salinity hazard, total dissolved solids, total hardness, residual sodium carbonate, and Kelly index, were found above the recommended standard in some water samples. The irrigation water quality index, which is a comprehensive analysis of five key parameters, also indicates that while some water sources require lower to moderate restriction, most of the groundwater sources require high to severe restriction for use. The spatial analysis revealed clear variations in water quality across the study area, identifying zones that may pose risks to soil structure and crop productivity.

The study further demonstrates that the IWQI-GIS framework is a robust and scalable tool for assessing irrigation water quality and understanding its spatial distribution in semi-arid areas. These findings highlight the necessity for targeted water management strategies in areas with elevated risks, which may include selective irrigation, blending of water sources, or monitoring sensitive zones. By providing a clear picture of water quality and its spatial patterns, this approach can guide local planners and policymakers in promoting sustainable irrigation practices and safeguarding groundwater resources.

## References

- Abadi HT, Alemayehu T, Berhe BA. 2024. Assessing the suitability of water for irrigation purposes using irrigation water quality indices in the Irob catchment, Tigray, Northern Ethiopia. *Water Quality Research Journal*, 60(1): 177–195. DOI: [10.2166/wqrj.2024.055](https://doi.org/10.2166/wqrj.2024.055).
- Abebe A, Jothimani M, Berhanu G. 2024. Hydrogeochemical evaluation of groundwater quality and its applicability for various purposes in the drought-prone Konso zone, rift valley, Southern Ethiopia. *Applied and Environmental Soil Science*, 2024(1): 7304847.

- Adimalla N, Dhakate R, Kasarla A, et al. 2020. Appraisal of groundwater quality for drinking and irrigation purposes in Central Telangana, India. *Groundwater for Sustainable Development*, 10: 100334. DOI: [10.1016/j.gsd.2020.100334](https://doi.org/10.1016/j.gsd.2020.100334).
- Aida HB, Vahid N, Zohre K, et al. 2024. Assessment of water quality suitability for agriculture in a potentially leachate-contaminated region. *Journal of Groundwater Science and Engineering*, 12(3): 281–292. DOI: [10.26599/JGSE.2024.9280021](https://doi.org/10.26599/JGSE.2024.9280021).
- Alemayehu T, Leis A, Eisenhauer A, et al. 2011. Multi-proxy approach ( $^2\text{H}/\text{H}$ ,  $^{18}\text{O}/^{16}\text{O}$ ,  $^{13}\text{C}/^{12}\text{C}$  and  $^{87}\text{Sr}/^{86}\text{Sr}$ ) for the evolution of carbonate-rich groundwater in basalt dominated aquifer of the Axum area, northern Ethiopia. *Geochemistry*, 71(2): 177–187. DOI: [10.1016/j.chemer.2011.02.007](https://doi.org/10.1016/j.chemer.2011.02.007).
- APHA. 2011. Standard methods for the examination of water and wastewater. American Public Health Association, Water Environment Federation, Washington. DOI: [10.2105/ajph.51.6.940-a](https://doi.org/10.2105/ajph.51.6.940-a).
- Appelo CAJ, Postma D. 2004. Geochemistry, groundwater, and pollution. CRC Press.
- Ayers RS, Westcot DW. 1985. Water quality for agriculture. Rome: Food and Agriculture Organization of the United Nations, 29(174): 1–163. DOI: [10.18356/3d544dc3-en](https://doi.org/10.18356/3d544dc3-en).
- Batarseh M, Imreizeeq E, Tilev S, et al. 2021. Assessment of groundwater quality for irrigation in the arid regions using Irrigation Water Quality Index (IWQI) and GIS-Zoning maps: Case study from Abu Dhabi Emirate, UAE. *Groundwater for Sustainable Development*, 14: 100611. DOI: [10.1016/j.gsd.2021.100611](https://doi.org/10.1016/j.gsd.2021.100611).
- Bennett G. 2023. Assessment of temporal and spatial variability of irrigation groundwater quality on the flanks of Mount Meru, northern Tanzania. *Groundwater for Sustainable Development*, 20: 100880. DOI: [10.1016/j.gsd.2022.100880](https://doi.org/10.1016/j.gsd.2022.100880).
- Berhanu KG, Hatiye SD, Lohani TK. 2023. Coupling support vector machine and the irrigation water quality index to assess groundwater quality suitability for irrigation practices in the Tana sub-basin, Ethiopia. *Water Practice and Technology*, 18(4): 884–900. DOI: [10.2166/wpt.2023.055](https://doi.org/10.2166/wpt.2023.055).
- Berhe BA. 2020. Evaluation of groundwater and surface water quality suitability for drinking and agricultural purposes in Kombolcha town area, eastern Amhara region, Ethiopia. *Applied Water Science*, 10(6): 127. DOI: [10.1007/s13201-020-01210-6](https://doi.org/10.1007/s13201-020-01210-6).
- Berhe GT, Baartman JE, Veldwisch GJ, et al. 2022. Irrigation development and management practices in Ethiopia: A systematic review on existing problems, sustainability issues and future directions. *Agricultural Water Management*, 274: 107959. DOI: [10.1016/j.agwat.2022.107959](https://doi.org/10.1016/j.agwat.2022.107959).
- Berhea S, Letab S. 2015. Suitability assessment of water quality of assabol dam for irrigation fish culture and drinking purposes at erob wereda eastern Tigray. *International Journal of Science and Research*, 4(3): 1388–1394.
- Debela A. 2017. Characterization and classification of salt-affected soils and irrigation water at Bule Hora district, West Guji zone. *Journal of Environment and Earth Sciences*, 7(12): 1–8.
- Djafer KH, Aichour A, Metaiche M, et al. 2024. Groundwater quality assessment for drinking and irrigation purposes in Boumerdes Region, Algeria. *Journal of Groundwater Science and Engineering*, 12(4): 397–410. DOI: [10.26599/JGSE.2024.9280030](https://doi.org/10.26599/JGSE.2024.9280030).
- Doneen LD. 1975. Water quality for irrigated agriculture. Plants in saline environments. Berlin, Heidelberg: Springer Berlin Heidelberg: 56–76. DOI: [10.1007/978-3-642-80929-3\\_5](https://doi.org/10.1007/978-3-642-80929-3_5).
- El Bilali A, Taleb A. 2020. Prediction of irrigation water quality parameters using machine learning models in a semi-arid environment. *Journal of the Saudi Society of Agricultural Sciences*, 19(7): 439–451. DOI: [10.1016/j.jssas.2019.12.004](https://doi.org/10.1016/j.jssas.2019.12.004).
- El Osta M, Masoud M, Alqarawy A, et al. 2022. Groundwater suitability for drinking and irrigation using water quality indices and multivariate modeling in Makkah Al-Mukarramah province, Saudi Arabia. *Water*, 14(3): 483. DOI: [10.3390/w14030483](https://doi.org/10.3390/w14030483).
- El-Rawy M, Fathi H. 2023. Groundwater pollution sources and their quality in the Kingdom of Saudi Arabia: State of the Art. *Groundwater Quality and Geochemistry in Arid and*

- Semi-Arid Regions, 215–235. DOI: [10.1007/698\\_2023\\_1050](https://doi.org/10.1007/698_2023_1050).
- Eswar D, Karuppusamy R, Chellamuthu S. 2021. Drivers of soil salinity and their correlation with climate change. *Current Opinion in Environmental Sustainability*, 50: 310–318. DOI: [10.1016/j.cosust.2020.10.015](https://doi.org/10.1016/j.cosust.2020.10.015).
- Gad M, El-Safa A, Magda M, et al. 2021. Integration of water quality indices and multivariate modeling for assessing surface water quality in Qaroun Lake, Egypt. *Water*, 13(16): 2258. DOI: [10.3390/w13162258](https://doi.org/10.3390/w13162258).
- Gaikwad S, Gaikwad S, Meshram D, et al. 2020. Geochemical mobility of ions in groundwater from the tropical western coast of Maharashtra, India: Implications for groundwater quality. *Environment, Development and Sustainability*, 22: 2591–2624. DOI: [10.1007/s10668-019-00312-9](https://doi.org/10.1007/s10668-019-00312-9).
- Gebrehiwot M, Tafesse NT, Habtu S, et al. 2021. The contribution of groundwater to the salinization of reservoir-based irrigation systems. *Agronomy*, 11(3): 512. DOI: [10.3390/agronomy11030512](https://doi.org/10.3390/agronomy11030512).
- Geburu H, Gebreyohannes T, Hagos E. 2024. Evaluation of groundwater quality for irrigation purposes and impact of irrigation on water in Golina River Basin, Northern Ethiopia. *Momona, Ethiopian Journal of Science*, 16(1): 144–166. DOI: [10.4314/mejs.v16i1.8](https://doi.org/10.4314/mejs.v16i1.8).
- Gintamo B, Khan MA, Gulilat H, et al. 2022. Determination of the physicochemical quality of groundwater and its potential health risk for drinking in Oromia, Ethiopia. *Environmental Health Insights*, 16: 11786302221096051. DOI: [10.1177/11786302221096051](https://doi.org/10.1177/11786302221096051).
- Gurmessa SK, MacAllister DJ, White D, et al. 2022. Assessing groundwater salinity across Africa. *Science of the Total Environment*, 828: 154283. DOI: [10.1016/j.scitotenv.2022.154283](https://doi.org/10.1016/j.scitotenv.2022.154283).
- Habtu S, Erkossa T, Froebrich J, et al. 2020. Integrating participatory data acquisition and modelling of irrigation strategies to enhance water productivity in a small-scale irrigation scheme in Tigray, Ethiopia. *Irrigation and Drainage*, 69: 23–37. DOI: [10.1002/ird.2235](https://doi.org/10.1002/ird.2235).
- Hagos M, Gebreyohannes T, Amare K, et al. 2020. Tectonic link between the Neoproterozoic dextral shear fabrics and Cenozoic extension structures of the Mekelle basin, Northern Ethiopia. *International Journal of Earth Sciences*, 109: 1957–1974. DOI: [10.1007/s00531-020-01882-0](https://doi.org/10.1007/s00531-020-01882-0).
- Hedjal S, Zouini D, Benamara A. 2018. Hydrochemical assessment of water quality for irrigation: A case study of the wetland complex of Guerbes-Sanhadja, North-East of Algeria. *Journal of Water and Land Development*, 38(VII-IX): 43–52. DOI: [10.2478/jwld-2018-0041](https://doi.org/10.2478/jwld-2018-0041).
- He ZJ, Fang LP, Liu CP, et al. 2025. A review of research progress on environmental fate and toxic effects of antibiotic-heavy metal co-contamination in soil-crop systems. *Rock and Mineral Analysis*, 44(4): 658–668. (in Chinese) DOI: [10.15898/j.ykcs.202501280014](https://doi.org/10.15898/j.ykcs.202501280014).
- Kebede L, Temesgen M, Fanta A, et al. 2023. Effect of locally adapted conservation tillage on runoff, soil erosion, and agronomic performance in semiarid rain-fed farming in Ethiopia. *Land*, 12(3): 593. DOI: [10.3390/land12030593](https://doi.org/10.3390/land12030593).
- Kumari D, Ranpariya KB, Davara MA, et al. 2022. Soil properties as influenced by the use of irrigation water having variable RSC and different varieties of groundnut (*Arachis hypogea* L.). *International Journal of Agricultural Sciences*, 18(2): 780–785. DOI: [10.15740/has/ijas/18.2/780-785](https://doi.org/10.15740/has/ijas/18.2/780-785).
- Kurniawan DA, Darmaji D, Astalini A, et al. 2023. A study of critical thinking skills, science process skills, and digital literacy: Reviewed based on gender. *Jurnal Penelitian Pendidikan IPA*, 9(4): 1741–1752. DOI: [10.29303/jppipa.v9i4.1644](https://doi.org/10.29303/jppipa.v9i4.1644).
- Masoud M, El Osta M, Alqarawy A, et al. 2022. Evaluation of groundwater quality for agriculture under different conditions using water quality indices, partial least squares regression models, and GIS approaches. *Applied Water Science*, 12(10): 244. DOI: [10.1007/s13201-022-01770-9](https://doi.org/10.1007/s13201-022-01770-9).
- Mehari H, Hailu B. 2019. Groundwater characterization of Raya Valley for irrigation use: The case of Mehoni Agricultural Research Center/Fachagama Experimental Site, Northern Ethiopia. *International Journal of Novel*

- Research in Life Science, 6(5): 46–52.
- Meireles ACM, Andrade EMD, Chaves LCG, et al. 2010. A new proposal for the classification of irrigation water. *Revista Ciência Agrônômica*, 41: 349–357. DOI: [10.1590/s1806-66902010000300005](https://doi.org/10.1590/s1806-66902010000300005).
- Mkumbo NJ, Mussa KR, Mariki EE, et al. 2022. The use of the DRASTIC-LU/LC model for assessing groundwater vulnerability to nitrate contamination in Morogoro Municipality, Tanzania. *Earth*, 3(4): 1161–1184. DOI: [10.3390/earth3040067](https://doi.org/10.3390/earth3040067).
- Mukiza P, Bazimenyera JDD, Nkundabose JP, et al. 2021. Assessment of irrigation water quality parameters of Nyandungu Wetlands. *Journal of Geoscience and Environment Protection*, 9(10): 151–160. DOI: [10.4236/gep.2021.910011](https://doi.org/10.4236/gep.2021.910011).
- Mutemi M, Njenga M, Lamond G, et al. 2017. Using local knowledge to understand challenges and opportunities for enhancing agricultural productivity in Western Kenya. *Sustainable Intensification in Smallholder Agriculture*: 177–195. DOI: [10.4324/9781315618791-12](https://doi.org/10.4324/9781315618791-12).
- Nedaw D. 2010. Water balance and groundwater quality of the Koraro area, Tigray, Northern Ethiopia. *Momona, Ethiopian Journal of Science*, 2(2): 110–127. DOI: [10.4314/mejs.v2i2.57678](https://doi.org/10.4314/mejs.v2i2.57678).
- Paliwal KV, Gandhi AP. 1976. Effect of salinity, SAR, Ca: Mg ratio in irrigation water, and soil texture on the predictability of exchangeable sodium percentage. *Soil Science*, 122(2): 85–90. DOI: [10.1097/00010694-197608000-00004](https://doi.org/10.1097/00010694-197608000-00004).
- Palmate SS, Kumar S, Poulouse T, et al. 2022. Comparing the effect of different irrigation water scenarios on an arid region pecan orchard using a system dynamics approach. *Agricultural Water Management*, 265: 107547. DOI: [10.1016/j.agwat.2022.107547](https://doi.org/10.1016/j.agwat.2022.107547).
- Richards LA. 1954. *Diagnosis and improvement of saline and alkali soils*. US Government Printing Office. DOI: [10.2134/agronj1954.00021962004600060019x](https://doi.org/10.2134/agronj1954.00021962004600060019x).
- Robinove CJ, Langford RH, Brookhart JW. 1958. *Saline-water resources of North Dakota (Vol. 1428)*. US Government Printing Office. DOI: [10.3133/wsp1428](https://doi.org/10.3133/wsp1428).
- Saad Eddin MR, Hassan AM, Hegazi AA, et al. 2023. Effects of root watering system on yield, water use efficiency, and fruit quality of date palm (cv Siwi): A case study in the arid climate, Egypt. *Irrigation Science*, 41(5): 589–601. DOI: [10.1007/s00271-022-00840-9](https://doi.org/10.1007/s00271-022-00840-9).
- Shitu K, Hymiro A, Tesfaw M. 2022. Review on baste soil improving approaches for waterlogging and soil salinization problems in agricultural land of Ethiopia. *Soil Water Science*, 6: 229–235. DOI: [10.36959/624/449](https://doi.org/10.36959/624/449).
- Subramanian T, Raj Mohan N, Elango L. 2010. Groundwater geochemistry and identification of hydrogeochemical processes in a hard rock region, southern India. *Environmental Monitoring and Assessment*, 162: 123–137. DOI: [10.1007/s10661-009-0781-4](https://doi.org/10.1007/s10661-009-0781-4).
- Swistock B. 2016. *Interpreting irrigation water tests*. Penn State Extension.
- Tadesse N, Bairu A, Bheemalingeswara K. 2011. Suitability of groundwater quality for irrigation with reference to hand-dug Wells, Hantebet Catchment, Tigray, Northern Ethiopia. *Momona Ethiopian Journal of Science*, 3(2): 31–47. DOI: [10.4314/mejs.v3i2.67711](https://doi.org/10.4314/mejs.v3i2.67711).
- Tadesse N, Bheemalingeswara K, Berhane A. 2009. Groundwater suitability for irrigation: A case study from Debre Kidane Watershed, Eastern Tigray, Ethiopia. *Momona Ethiopian Journal of Science*, 1(1): 36–58. DOI: [10.4314/mejs.v1i1.46040](https://doi.org/10.4314/mejs.v1i1.46040).
- Tarolli P, Luo J, Park E, et al. 2024. Soil salinization in agriculture: Mitigation and adaptation strategies combining nature-based solutions and bioengineering. *Iscience*, 27(2): 1–9. DOI: [10.1016/j.isci.2024.108830](https://doi.org/10.1016/j.isci.2024.108830).
- Tegegne AM, Lohani TK, Eshete AA. 2023. Evaluation of groundwater quality for drinking and irrigation purposes using proxy indices in the Gunabay watershed, Upper Blue Nile Basin, Ethiopia. *Heliyon*, 9(4): e15263. DOI: [10.1016/j.heliyon.2023.e15263](https://doi.org/10.1016/j.heliyon.2023.e15263).
- Tian XH, Jia LL, Luo JX. 2025. Hydrochemical characteristics and water-quality evaluation of groundwater in the Ziya River Plain, Hai River Basin. *Rock and Mineral Analysis*, 44(4): 735–746. (in Chinese) DOI: [10.15898/j.ykcs.202411180236](https://doi.org/10.15898/j.ykcs.202411180236).
- Tomaz A, Palma P, Fialho S, et al. 2020. Spatial

- and temporal dynamics of irrigation water quality under drought conditions in a large reservoir in Southern Portugal. *Environmental Monitoring and Assessment*, 192: 1–17. DOI: [10.1007/s10661-019-8048-1](https://doi.org/10.1007/s10661-019-8048-1).
- Vasanthavigar M, Srinivasamoorthy K, Prasanna MV. 2013. Identification of groundwater contamination zones and its sources by using the multivariate statistical approach in the Thirumanimuttar sub-basin, Tamil Nadu, India. *Environmental Earth Sciences*, 68: 1783–1795. DOI: [10.1007/s12665-012-1868-8](https://doi.org/10.1007/s12665-012-1868-8).
- Wahyuningsih S, Novita E, Ramadhan RN. 2023. Determination of suitable plant types in an irrigation command area using the IWQI Method. *Jurnal Takin Pertanian Lampung (Journal of Agricultural Engineering)*, 12(4): 795. DOI: [10.23960/jtep-l.v12i4.795-806](https://doi.org/10.23960/jtep-l.v12i4.795-806).
- Wilcox L. 1955. Classification and use of irrigation waters (No. 969). US Department of Agriculture.
- Woldemariyam F, Ayenew T. 2016. Identification of hydrogeochemical processes in groundwater of Dawa River basin, southern Ethiopia. *Environmental Monitoring and Assessment*, 188(8): 481. DOI: [10.1007/s10661-016-5480-3](https://doi.org/10.1007/s10661-016-5480-3).
- Zhou H, Shi H, Yang Y, et al. 2024. Insights into plant salt stress signaling and tolerance. *Journal of Genetics and Genomics*, 51(1): 16–34. DOI: [10.1016/j.jgg.2023.08.007](https://doi.org/10.1016/j.jgg.2023.08.007).
- Zhu M, Wang S, Kong X, et al. 2019. Interaction of surface water and groundwater influenced by groundwater over-extraction, wastewater discharge, and water transfer in Xiong'an New Area, China. *Water*, 11(3): 539. DOI: [10.3390/w11030539](https://doi.org/10.3390/w11030539).